Cosmic-ray Electrons at GeV—TeV energies and CALET

Nicholas Cannady

ISCRA 2022

Erice, Italy

Motivation

Cosmic-ray (CR) electrons are a unique species that can tell us about:

- Nearby sources of high-energy electrons
- Diffusion and energy loss in the Galaxy
- Dark matter

Motivation

Cosmic-ray (CR) electrons are a unique species that can tell us about:

- Nearby sources of high-energy electrons
- Diffusion and energy loss in the Galaxy
- Dark matter

Their transport through the Galaxy can be described by the diffusion equation:

$$\frac{dN(E)}{dt} = D(E)\nabla^2 N(E) + \frac{\partial}{\partial E}[b(E)N(E)] + Q(E)$$

Motivation

Cosmic-ray (CR) electrons are a unique species that can tell us about:

- Nearby sources of high-energy electrons
- Diffusion and energy loss in the Galaxy
- Dark matter

Their transport through the Galaxy can be described by the diffusion equation:

$$\frac{dN(E)}{dt} = D(E)\nabla^2 N(E) + \frac{\partial}{\partial E}[b(E)N(E)] + Q(E)$$

diffusion term

energy loss term

source term

Energetic electrons are affected by the Galactic magnetic field, scrambling their directions

Electrons lose energy in transport via
Ionization
Bremsstrahlung
Adiabatic cooling
Synchrotron emission
Inverse Compton effect

Injection from the accelerator. Tends to follow a power law spectrum with some high-energy cutoff

Steady-state solution

Assuming an input power law of the form

$$Q(E) = KE^{-\alpha}$$

if we find a solution for a steady state such that

$$\frac{dN}{dt} = 0 \quad \text{and} \quad \nabla^2 N(E) = 0,$$

we find that

$$-\frac{\partial}{\partial E}[b(E)N(E)] = KE^{-\alpha}$$

or

$$N(E) = \frac{KE^{-(\alpha-1)}}{(\alpha-1)}\frac{1}{b(E)}$$

Steady-state solution

Assuming an input power law of the form $$Q(E) = KE^{-\alpha}$$

if we find a solution for a steady state such that $\frac{dN}{dt} = 0$ and $\nabla^2 N(E) = 0$,

we find that $$-\frac{\partial}{\partial E}[b(E)N(E)] = KE^{-\alpha}$$

or $$N(E) = \frac{KE^{-(\alpha-1)}}{(\alpha-1)}\frac{1}{b(E)}$$

If the dominant energy loss is due to…	…then for our loss term,	…and the spectral shape after propagation is…
Ionization	$b(E) \propto \ln(\frac{E}{m_e c^2})$	$N(E) \approx K'E^{-(\alpha-1)}$
Bremsstrahlung Adiabatic cooling	$b(E) \propto E$	$N(E) \approx K'E^{-\alpha}$
Synchrotron Inverse Compton	$b(E) \propto E^2$	$N(E) \approx K'E^{-(\alpha+1)}$

Steady-state solution

Assuming an input power law of the form $$Q(E) = KE^{-\alpha}$$

if we find a solution for a steady state such that $$\frac{dN}{dt} = 0 \quad \text{and} \quad \nabla^2 N(E) = 0,$$

we find that $$-\frac{\partial}{\partial E}[b(E)N(E)] = KE^{-\alpha}$$

or $$N(E) = \frac{KE^{-(\alpha-1)}}{(\alpha-1)} \frac{1}{b(E)}$$

Assuming injection spectrum, observed flux vs. energy tells us about significant energy loss processes

If the dominant energy loss is due to...	...then for our loss term,	...and the spectral shape after propagation is...
Ionization	$b(E) \propto \ln(\frac{E}{m_e c^2})$	$N(E) \approx K'E^{-(\alpha-1)}$
Bremsstrahlung Adiabatic cooling	$b(E) \propto E$	$N(E) \approx K'E^{-\alpha}$
Synchrotron Inverse Compton	$b(E) \propto E^2$	$N(E) \approx K'E^{-(\alpha+1)}$

Characteristic scales for high-energy CR electrons

Beyond the accelerator, relatively little material is traversed

- Synchrotron and inverse Compton dominate

$$\frac{dE}{dt} = AE^2 \qquad (A \approx 5 \times 10^{-9} GeV^{-1} yr^{-1})$$

Characteristic electron lifetime in this regime:

$$\frac{\Delta E}{\tau} = AE^2 \xrightarrow{\Delta E \,\to\, 0.5E} \tau = \frac{1}{2AE}$$

Characteristic scales for high-energy CR electrons

Beyond the accelerator, relatively little material is traversed

- Synchrotron and inverse Compton dominate

$$\frac{dE}{dt} = AE^2 \qquad (A \approx 5 \times 10^{-9} GeV^{-1} yr^{-1})$$

Characteristic electron lifetime in this regime:

$$\frac{\Delta E}{\tau} = AE^2 \xrightarrow{\Delta E \to 0.5E} \tau = \frac{1}{2AE}$$

Corresponding diffusion length:

$$R = \sqrt{2D\tau} = \sqrt{\frac{D}{AE}} \qquad D \approx (1-4) \times \begin{pmatrix} 1 \times 10^{28} cm^2 s^{-1} \\ 3.5 \times 10^{-8} kpc^2 yr^{-1} \end{pmatrix} \times \left(\frac{E}{1\ GeV}\right)^{0.3}$$

Characteristic scales for high-energy CR electrons

Beyond the accelerator, relatively little material is traversed

- Synchrotron and inverse Compton dominate

$$\frac{dE}{dt} = AE^2 \qquad (A \approx 5 \times 10^{-9} GeV^{-1} yr^{-1})$$

Characteristic electron lifetime in this regime:

$$\frac{\Delta E}{\tau} = AE^2 \xrightarrow{\Delta E \to 0.5E} \tau = \frac{1}{2AE}$$

Corresponding diffusion length:

$$R = \sqrt{2D\tau} = \sqrt{\frac{D}{AE}} \qquad D \approx (1-4) \times \begin{pmatrix} 1 \times 10^{28} cm^2 s^{-1} \\ 3.5 \times 10^{-8} kpc^2 yr^{-1} \end{pmatrix} \times \left(\frac{E\ V}{1\ GeV}\right)^{0.3}$$

Plugging in some numbers,

$$\tau = \frac{1}{2AE} = (1 \times 10^5 yr)\left(\frac{E\ V}{1\ TeV}\right)^{-1} \qquad R = \sqrt{2D\tau} = (0.25 - 1\ kpc) \times \left(\frac{E\ V}{1\ TeV}\right)^{-0.35}$$

Characteristic scales for high-energy CR electrons

Beyond the accelerator, relatively little material is traversed

- Synchrotron and inverse Compton dominate

$$\frac{dE}{dt} = AE^2 \qquad (A \approx 5 \times 10^{-9} GeV^{-1} yr^{-1})$$

Characteristic electron lifetime in this regime:

$$\frac{\Delta E}{\tau} = AE^2 \xrightarrow{\Delta E \to 0.5E} \tau = \frac{1}{2AE}$$

Corresponding diffusion length:

$$R = \sqrt{2D\tau} = \sqrt{\frac{D}{AE}} \qquad D \approx (1-4) \times \left(\frac{1 \times 10^{28} cm^2 s^{-1}}{3.5 \times 10^{-8} kpc^2 yr^{-1}} \right) \times \left(\frac{E}{1\ GeV} \right)^{0.3}$$

Plugging in some numbers,

$$\tau = \frac{1}{2AE} = (1 \times 10^5 yr) \left(\frac{E}{1\ TeV} \right)^{-1} \qquad R = \sqrt{2D\tau} = (0.25 - 1\ kpc) \times \left(\frac{E}{1\ TeV} \right)^{-0.35}$$

We will not see electrons above 1 TeV that were accelerated over 1 kpc away or over 10^5 years ago -> signatures of nearby sources

Acceleration of CR electrons

Cosmic rays up to <~ PeV energies → diffusive shock acceleration in SNRs

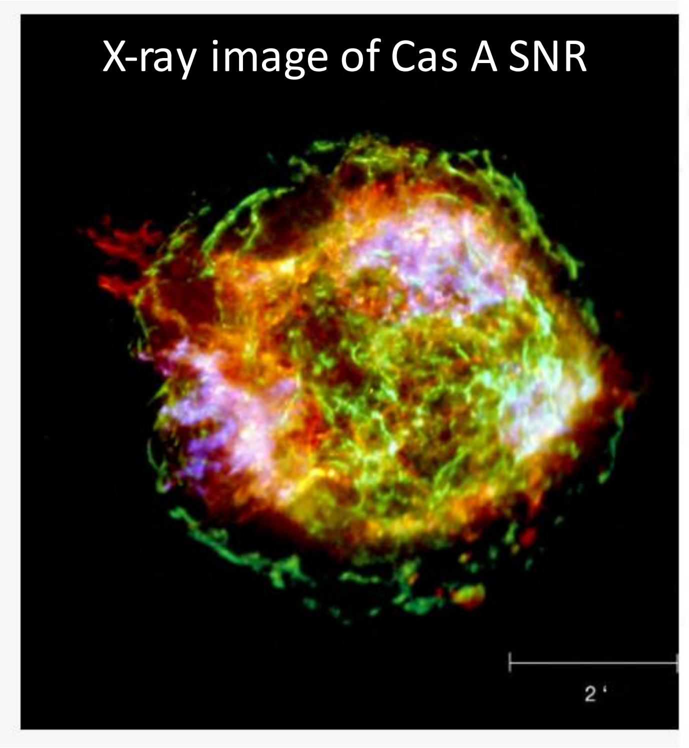

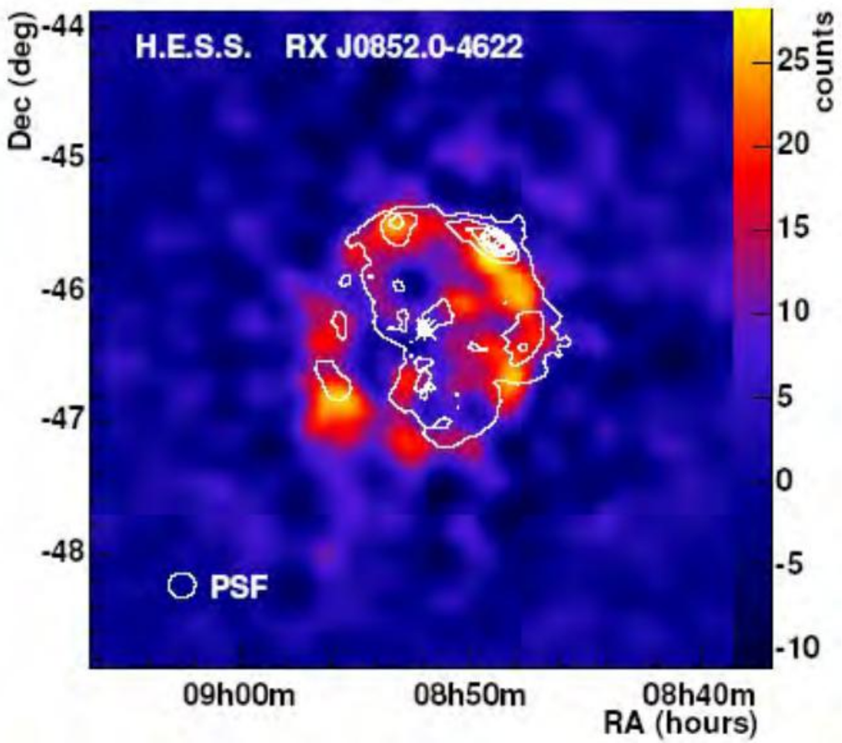

X-ray synchrotron emission supports presence of high-energy electrons in SNRs

Gamma-ray observations can fit models of electronic and/or hadronic particle acceleration

Variation of parameters in models

Diffusion coefficient

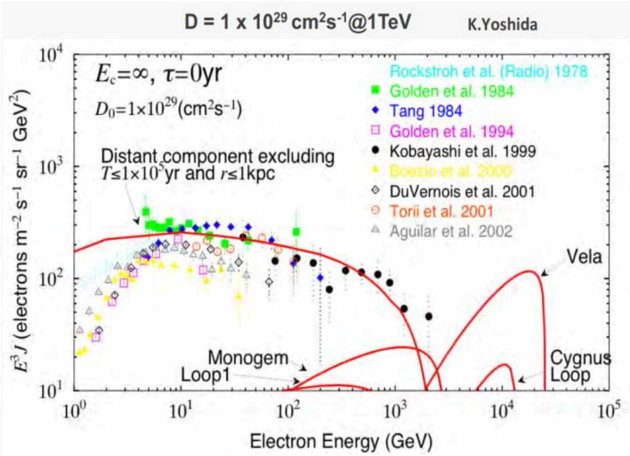

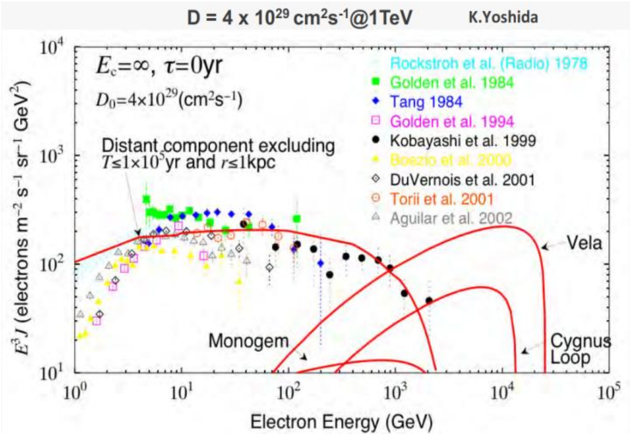

Features in the spectrum above 1 TeV could confirm a nearby accelerator and constrain source and propagation model parameters

Variation of parameters in models

Diffusion coefficient

Source cutoff energy

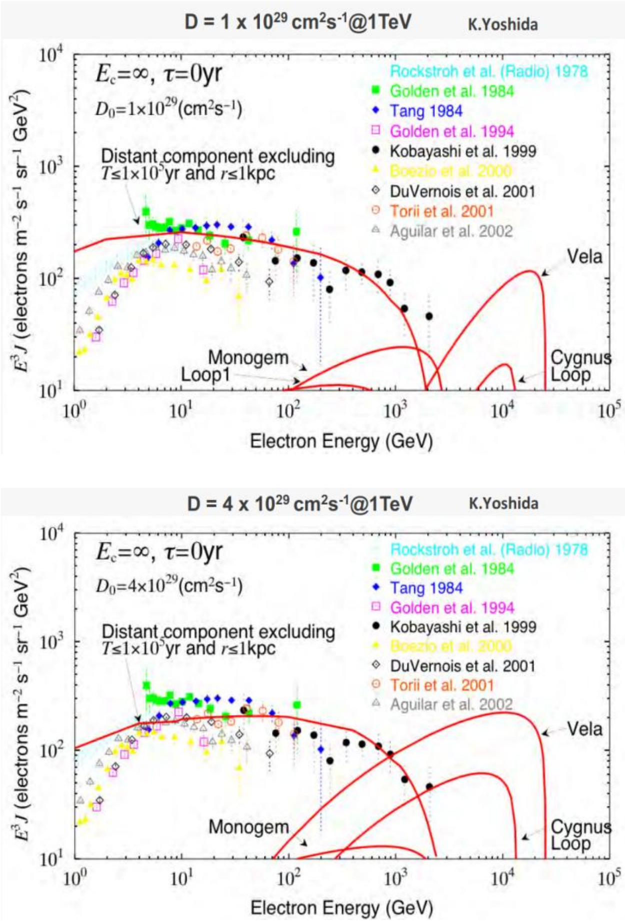

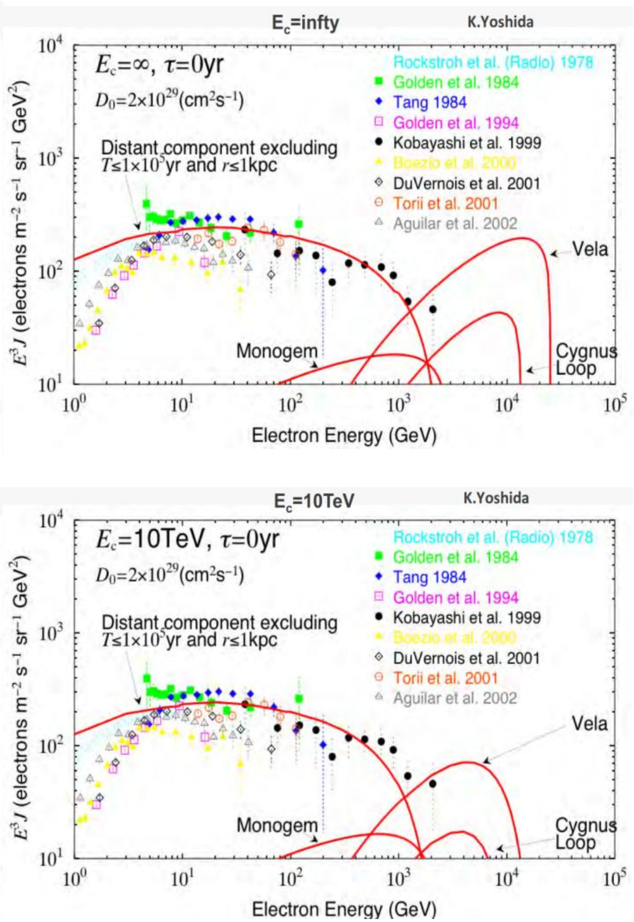

Features in the spectrum above 1 TeV could confirm a nearby accelerator and constrain source and propagation model parameters

Variation of parameters in models

Diffusion coefficient

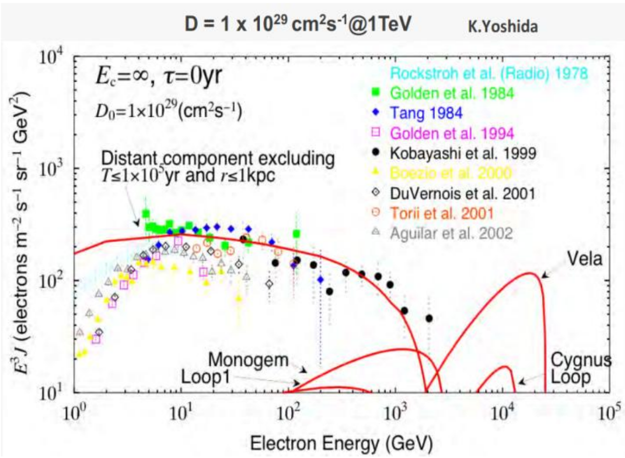

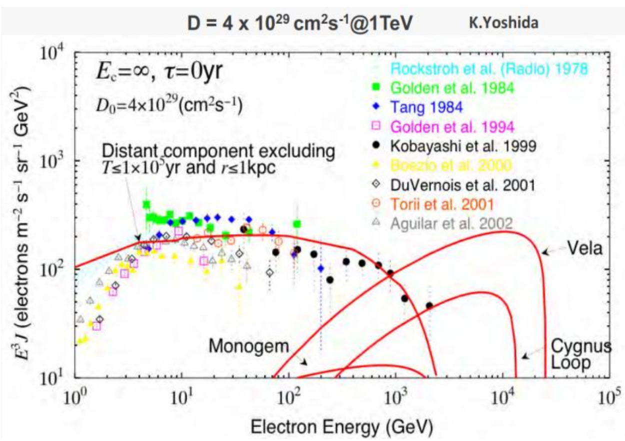

Source cutoff energy

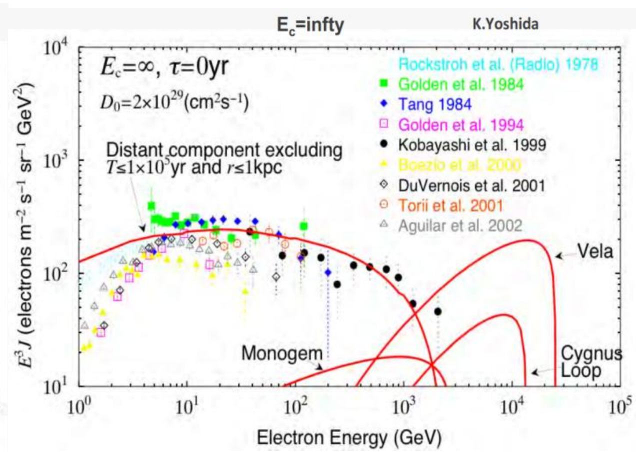

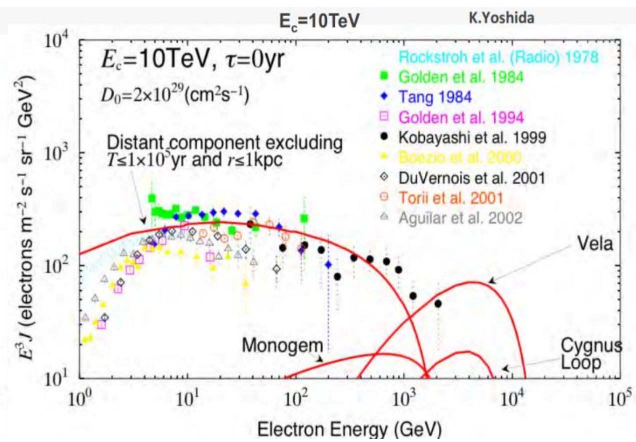

Time since SNR escape

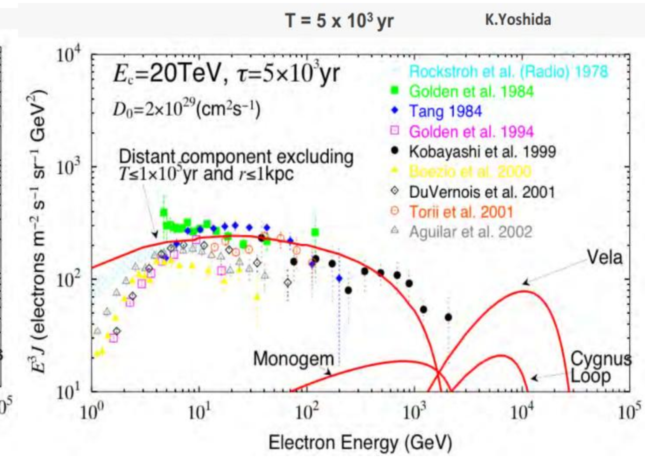

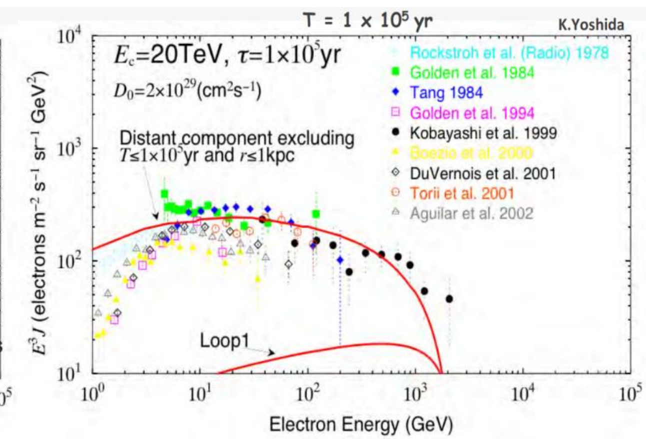

Features in the spectrum above 1 TeV could confirm a nearby accelerator and constrain source and propagation model parameters

Dark matter decay signatures?

Some dark matter candidate models include decay into leptonic channels, leading to features in the high-energy CR electron spectrum

Supersymmetric candidate

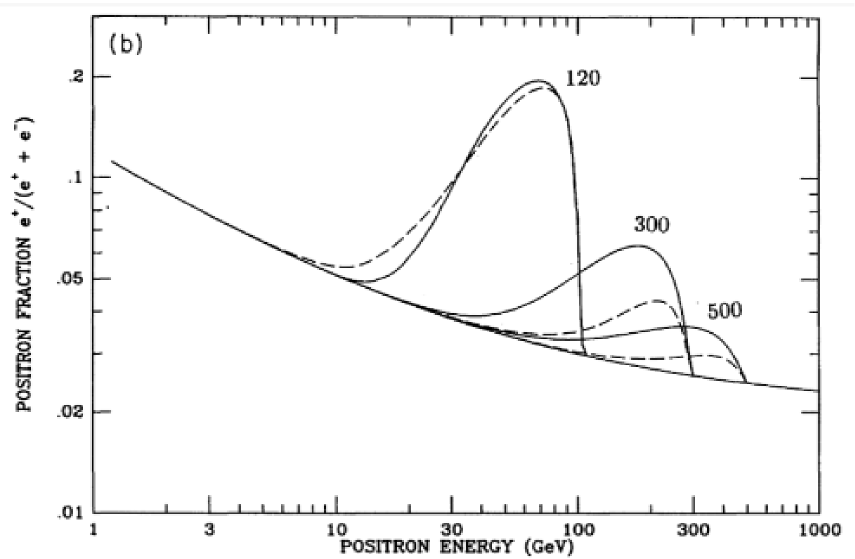

Kamionkowski et al. 1991

Kaluza-Klein candidate

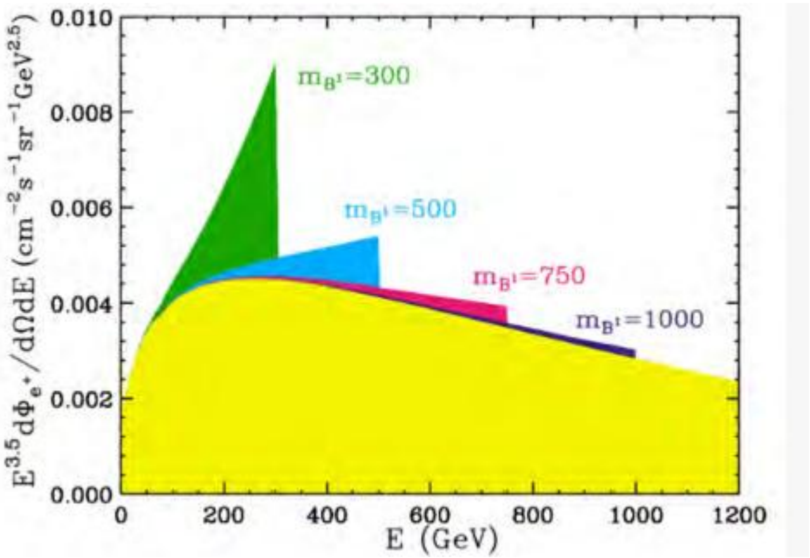

Cheng et al. 2002

Fine energy resolution necessary for the detection of line signals in a continuum

Experimental results from early instruments

The observation landscape in the mid-2000's had large variations between experiments

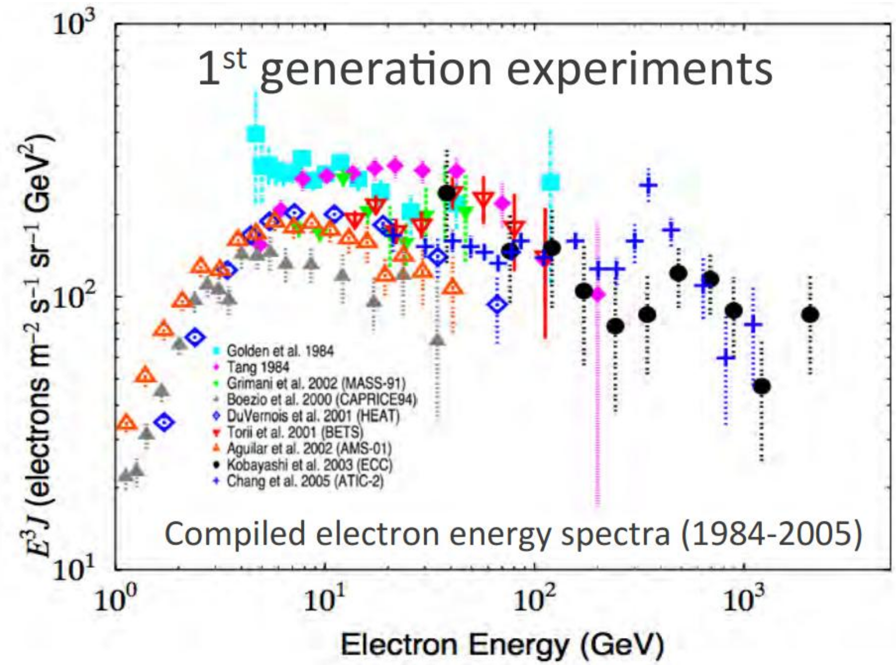

Experimental results from early instruments

The observation landscape in the mid-2000's had large variations between experiments

A feature consistently seen in the multiple flights of the ATIC detector was published in Nature in 2008 as a possible DM signature

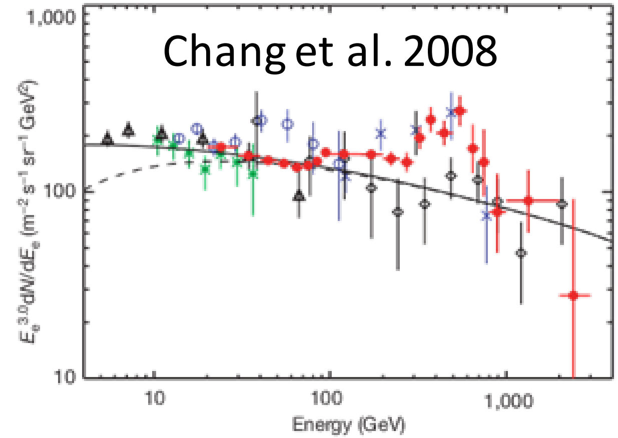

Figure 3 | ATIC results showing agreement with previous data at lower energy and with the imaging calorimeter PPB-BETS at higher energy. The electron differential energy spectrum measured by ATIC (scaled by E^3) at the top of the atmosphere (red filled circles) is compared with previous observations from the Alpha Magnetic Spectrometer AMS (green stars)[31], HEAT (open black triangles)[30], BETS (open blue circles)[32], PPB-BETS (blue crosses)[16] and emulsion chambers (black open diamonds)[4,8,9], with uncertainties of one standard deviation. The GALPROP code calculates a power-law spectral index of −3.2 in the low-energy region (solid curve)[14]. (The dashed curve is the solar modulated electron spectrum and shows that modulation is unimportant above ~20 GeV.) From several hundred to ~800 GeV, ATIC observes an 'enhancement' in the electron intensity over the GALPROP curve. Above 800 GeV, the ATIC data returns to the solid line.

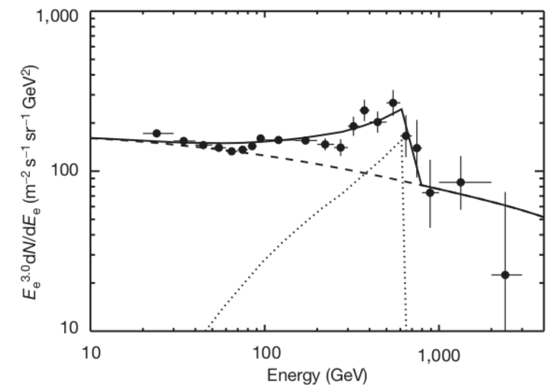

Figure 4 | Assuming an annihilation signature of Kaluza–Klein dark matter, all the data can be reproduced.

Experimental results from early instruments

The observation landscape in the mid-2000's had large variations between experiments

A feature consistently seen in the multiple flights of the ATIC detector was published in Nature in 2008 as a possible DM signature

A new generation of instruments was necessary to resolve the discrepancy between experiments and to confirm or reject this very significant result

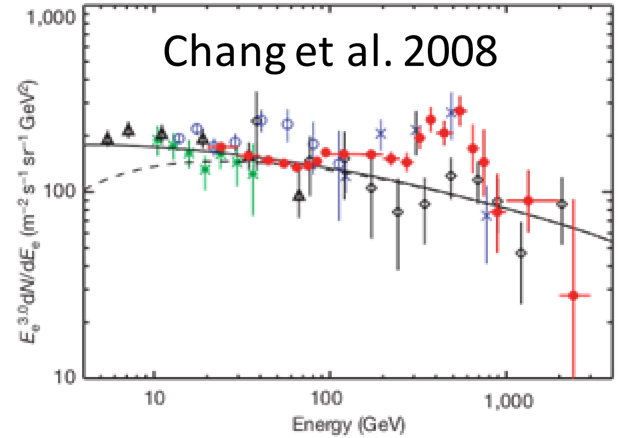

Figure 3 | ATIC results showing agreement with previous data at lower energy and with the imaging calorimeter PPB-BETS at higher energy. The electron differential energy spectrum measured by ATIC (scaled by E^3) at the top of the atmosphere (red filled circles) is compared with previous observations from the Alpha Magnetic Spectrometer AMS (green stars)[31], HEAT (open black triangles)[30], BETS (open blue circles)[32], PPB-BETS (blue crosses)[16] and emulsion chambers (black open diamonds)[4,8,9], with uncertainties of one standard deviation. The GALPROP code calculates a power-law spectral index of −3.2 in the low-energy region (solid curve)[14]. (The dashed curve is the solar modulated electron spectrum and shows that modulation is unimportant above ~20 GeV.) From several hundred to ~800 GeV, ATIC observes an 'enhancement' in the electron intensity over the GALPROP curve. Above 800 GeV, the ATIC data returns to the solid line.

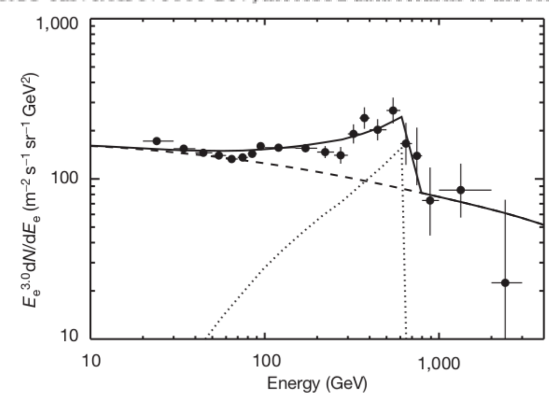

Figure 4 | Assuming an annihilation signature of Kaluza–Klein dark matter, all the data can be reproduced.

The Calorimetric Electron Telescope (CALET)

CALET is an ISS-borne instrument designed to study CR electrons

- Deep EM calorimeter (30 radiation lengths)
- Zenith pointing observations
- Advanced Stellar Compass star tracker for pointing knowledge
- CALET Gamma-Ray Burst Monitor (CGBM) sensitive to keV—MeV energy photons
- Deployed on Japanese Experiment Module – Exposed Facility (JEM-EF)
- Operational 2015—2024+

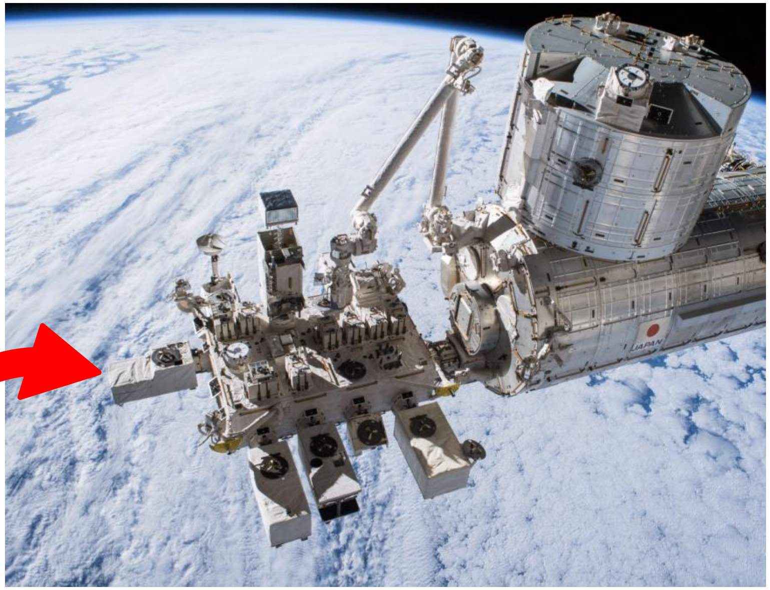

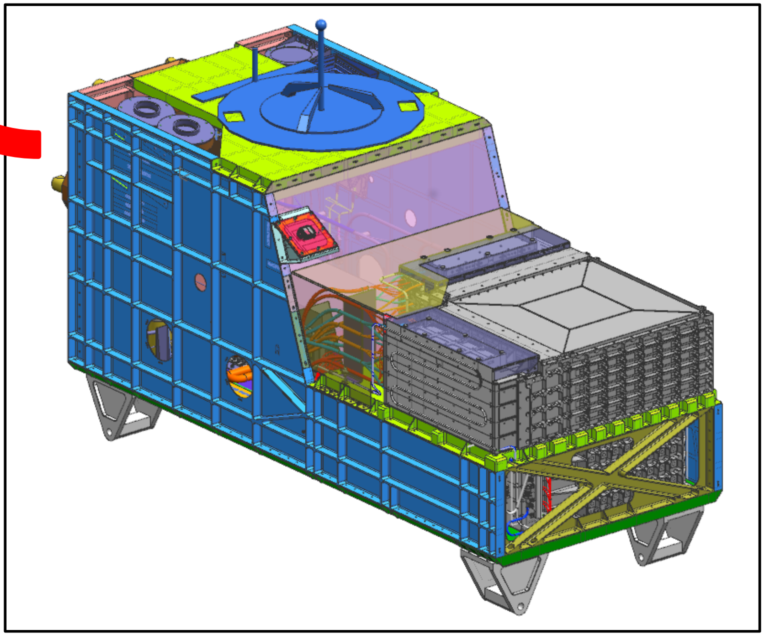

Electromagnetic Showers

- Electrons interact with matter by
  - Ionization
  - Bremsstrahlung
  - Annihilation (positrons)
- Photons interact with matter by
  - Photoabsorption
  - Compton scattering
  - Pair production

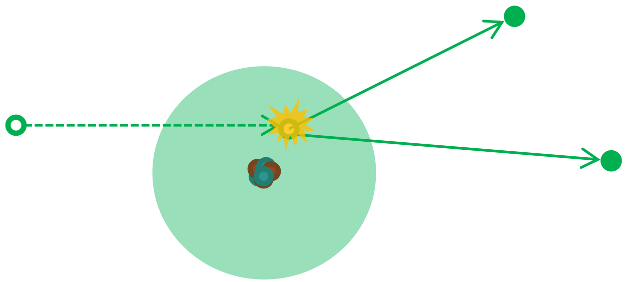

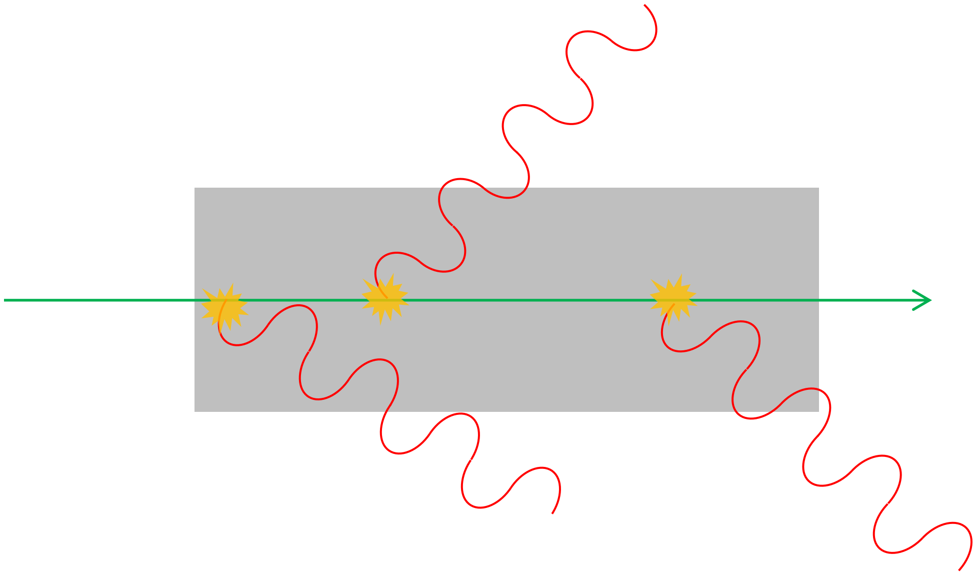

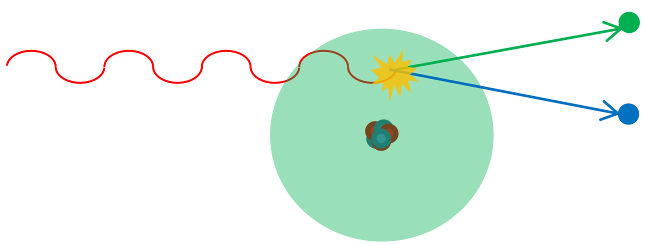

Electromagnetic Showers

- Electrons interact with matter by
  - Ionization
  - Bremsstrahlung
  - Annihilation (positrons)
- Photons interact with matter by
  - Photoabsorption
  - Compton scattering
  - Pair production
- For sufficiently high energies, processes produce a cascade
  - Multiplicity of interactions >1

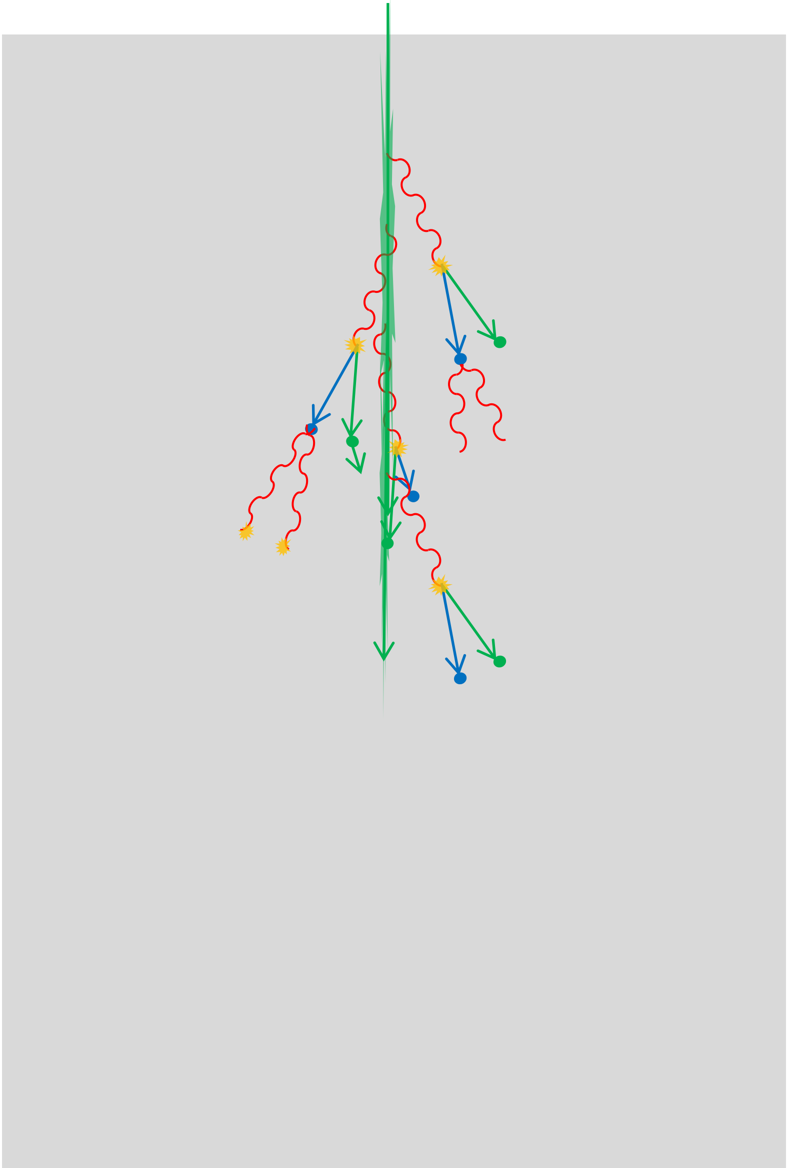

Electromagnetic Showers

- Electrons interact with matter by
  - Ionization
  - Bremsstrahlung
  - Annihilation (positrons)
- Photons interact with matter by
  - Photoabsorption
  - Compton scattering
  - Pair production
- For sufficiently high energies, processes produce a cascade
  - Multiplicity of interactions >1
  - Shower ends when average particle energy too low to produce energetic secondaries

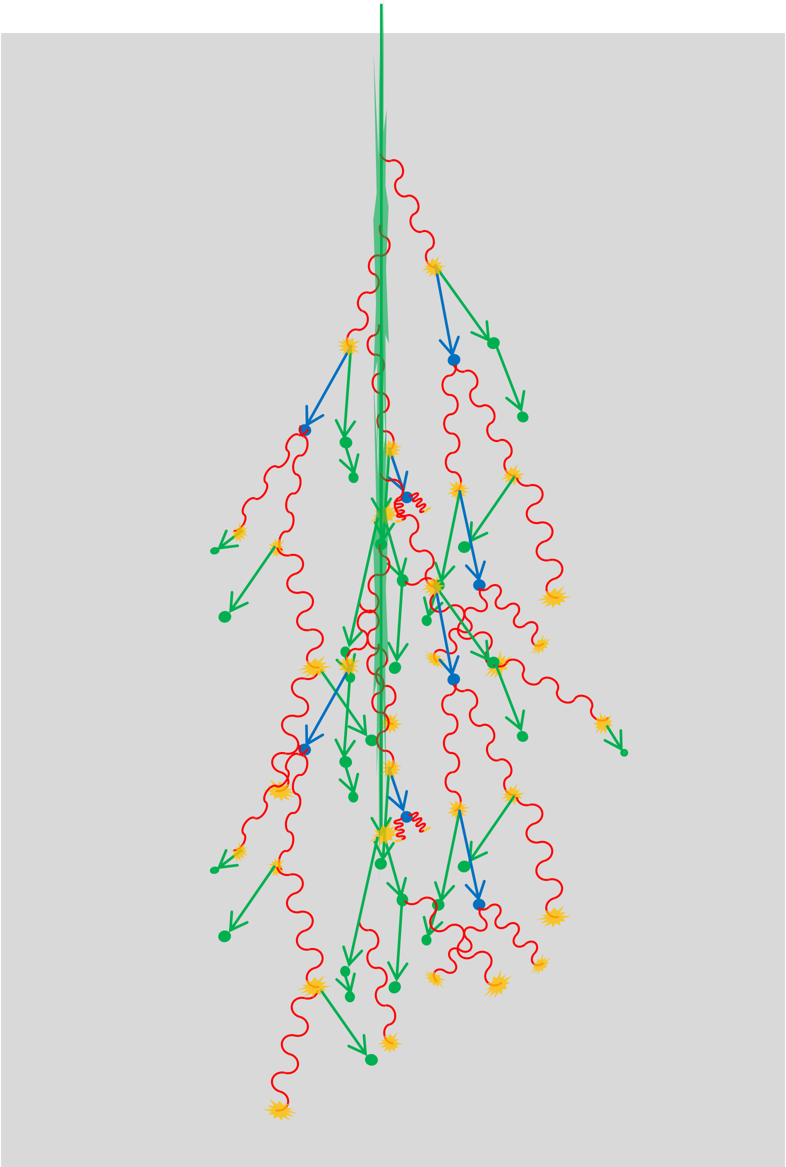

The CALET Calorimeter

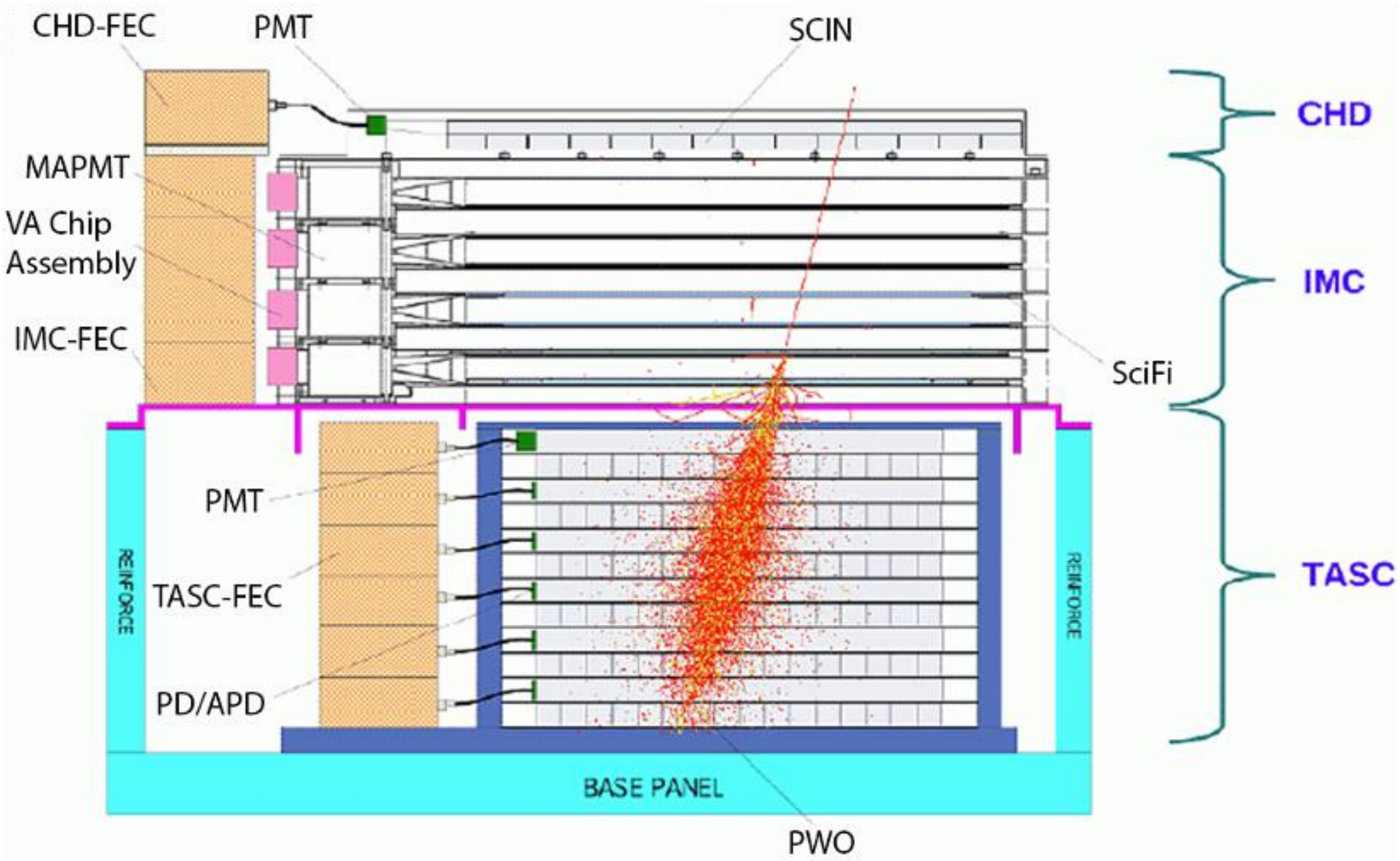

The CALET Calorimeter

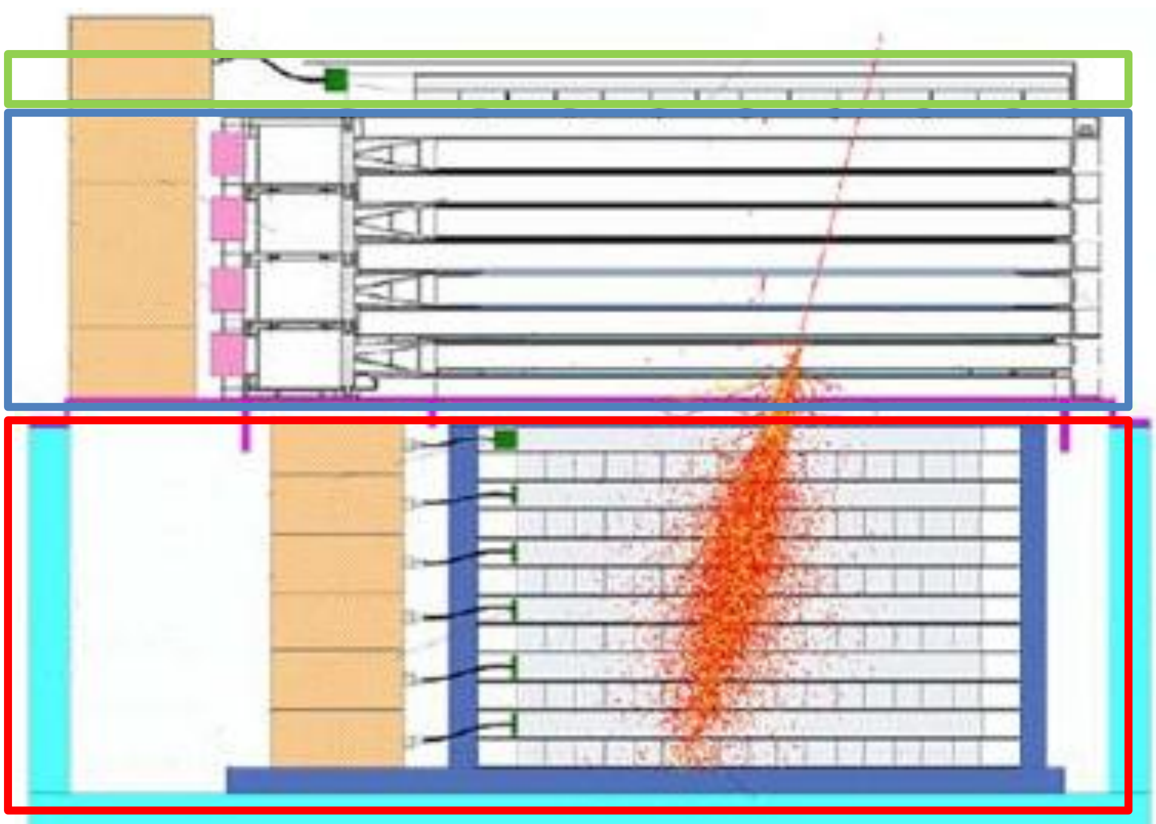

Image: simulated 1 TeV electron event in CALET

CHD – Charge Detector
- 2 x 14 plastic scintillating paddles
- Charge measurement Z = 0 → 40+

IMC – Imaging Calorimeter
- 8 x 2 x 448 plastic scintillating fibers
- 7 tungsten sheets
- Shower development and imaging
- 3 electron radiation lengths normal incidence depth

TASC – Total Absorption Calorimeter
- 6 x 2 x 16 lead tungstate logs
- Electromagnetic shower absorption
- 27 electron radiation lengths normal incidence depth

- **Geometrical Factor:**
  1040 cm^2 sr for electrons, light nuclei
  1000 cm^2 sr for gamma-rays
  4000 cm^{2}sr for ultra-heavy nuclei

- **ΔE/E:**
  ~2 % (>10GeV) for e , γ
  ~30-35% for hadrons

- **e/p separation:** ~10^5
- **Charge resolution:** 0.15-3 e (p-Fe)
- **Angular resolution:**
  0.2°for gamma-rays > ~50 GeV

Shower imaging with the IMC – a sampling calorimeter

Active material: plastic scintillating fibers (1 mm x 1mm cross section)
- Sensitive to energy deposit by ionization ($dE/dx \propto Z^2$ for MIPs)
- Snapshots of spatial distribution of energy deposit in shower
- Secondary charge measurement after CHD

Fibers not to scale for illustration

Real CALET IMC has ~4.5x more fibers

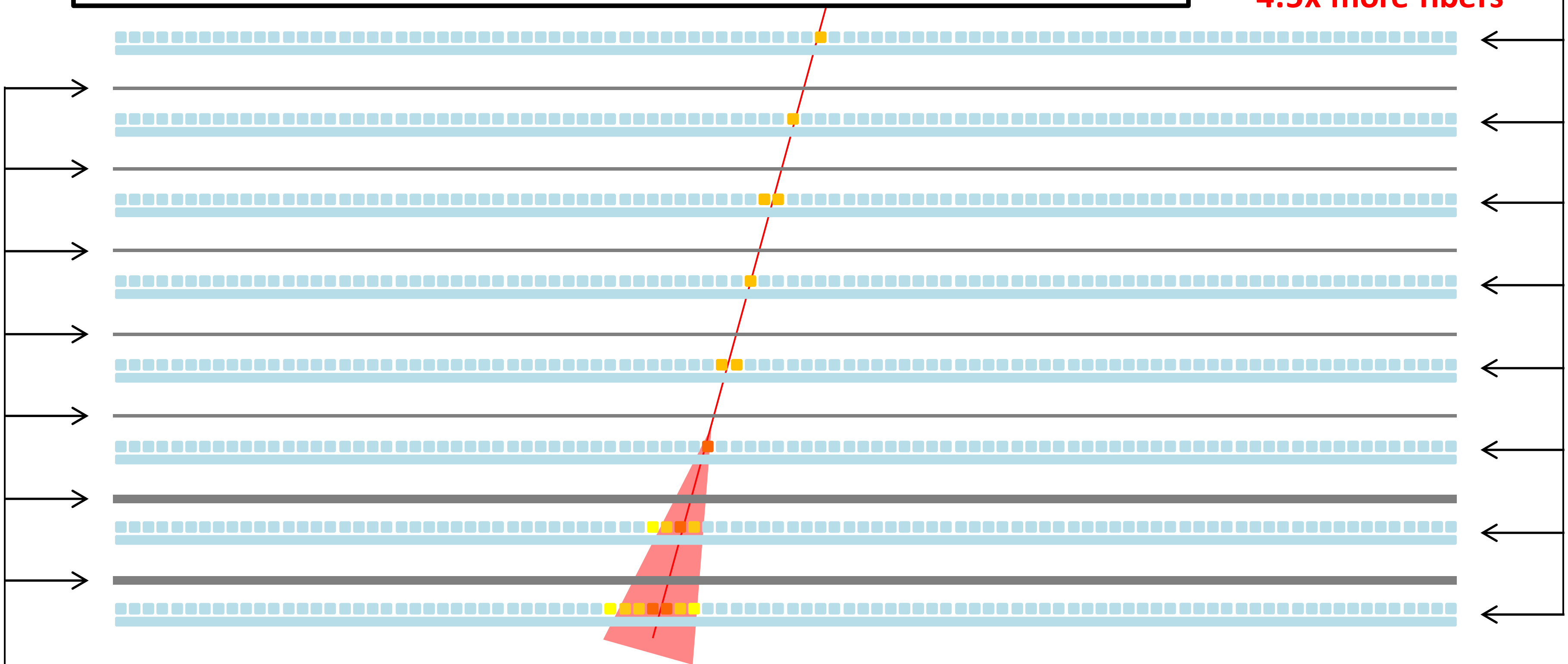

Passive material: tungsten sheets
- Stimulate shower development (first 5: 0.2 X_0 each; last two: 1 X_0 each)
- Promote first pair conversion for photon primaries
- Total depth at normal incidence = 3 X_0

X_0: "Radiation length" Characteristic energy loss distance for electron brems.

Showers in the TASC: a full absorption calorimeter

Fully active calorimeter: Lead Tungstate ($PbWO_4$)
- Dense, inorganic scintillator: lots of grammage for lots of stopping power
- Segmentation enables crude shower imaging for consistency checks with IMC reconstruction
- Fine energy deposit resolution → high fidelity electron energy reconstruction

Multiple gain ranges on each detector element

(2 on top layer, 4 on all others):

very wide dynamic range

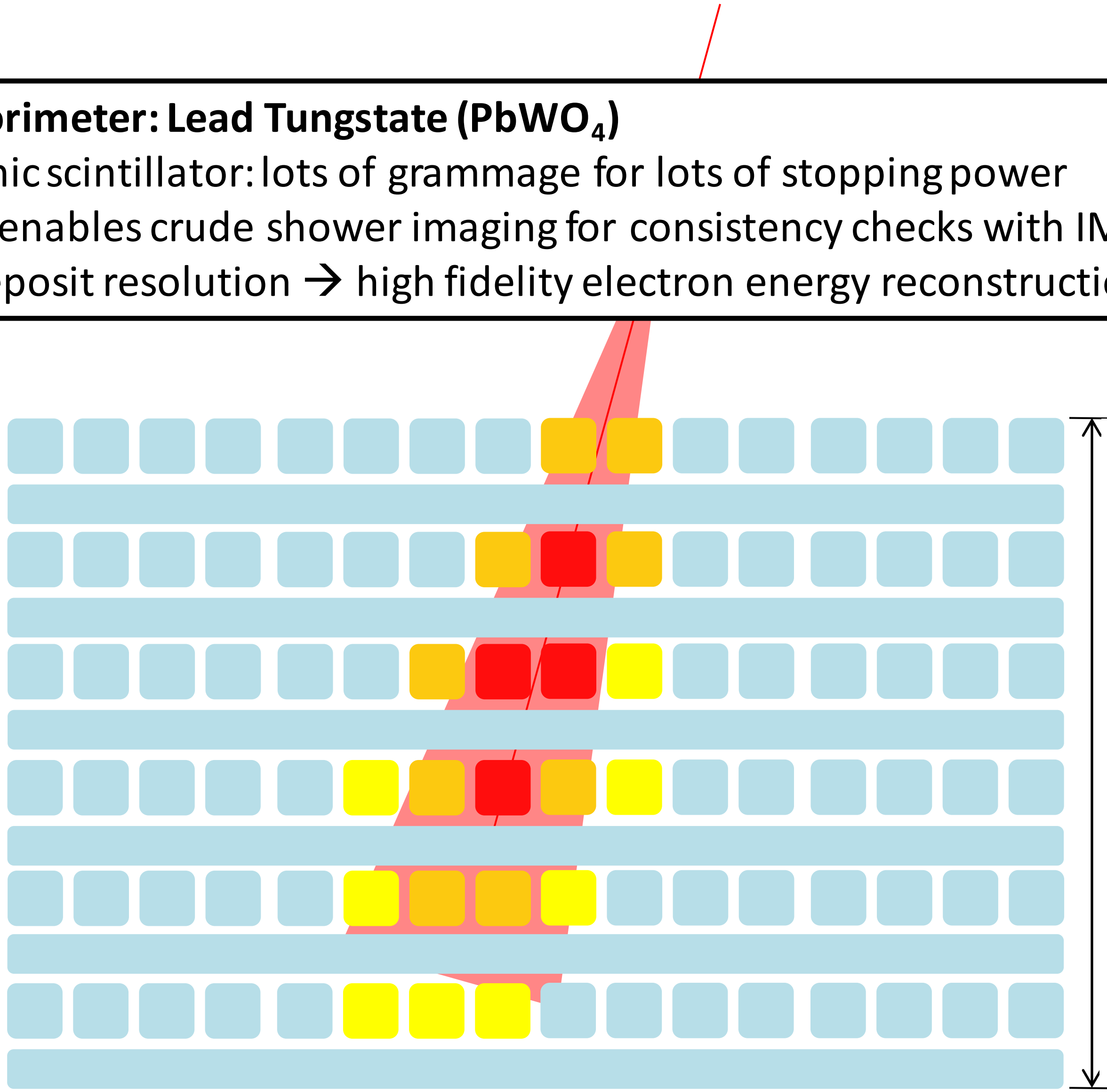

Normal incidence depth of 27 X_0: full EM shower containment up to TeV energies

Normal incidence depth of ~1 proton interaction length: only about 1 nuclear interaction in event for hadron primaries

Sample event in CALET: 250 GeV electron from flight data

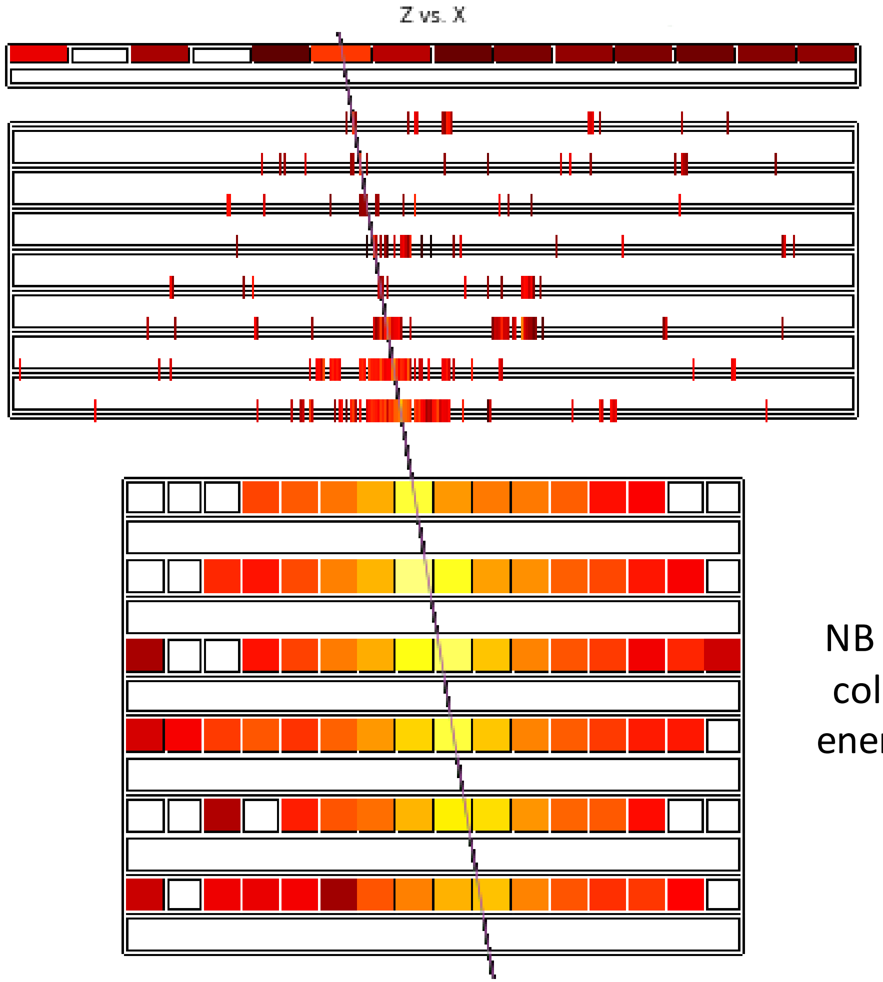

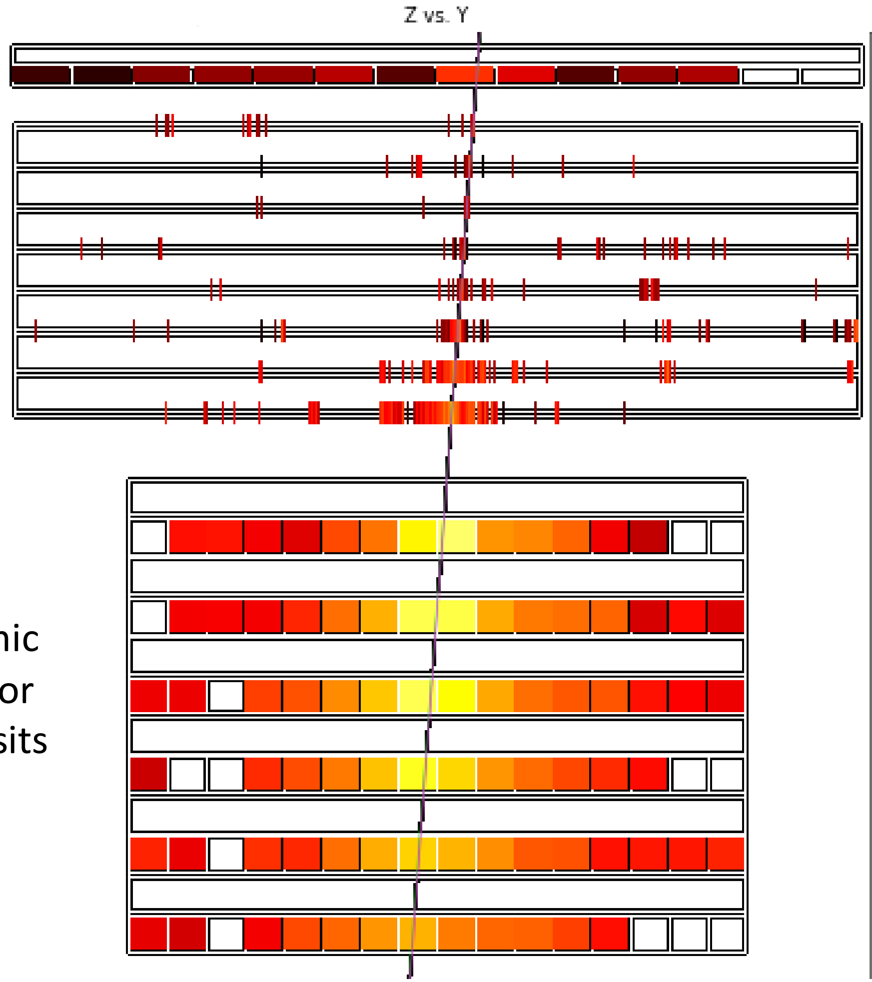

NB logarithmic color scale for energy deposits

CALET flight instrumentation, integration, and launch

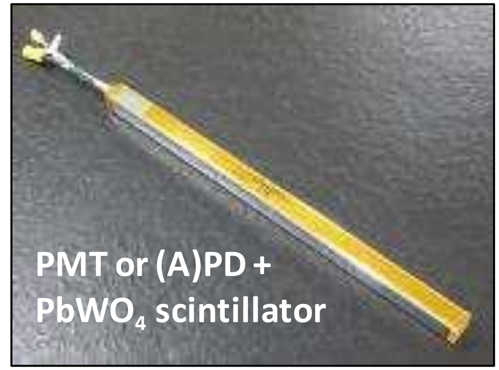

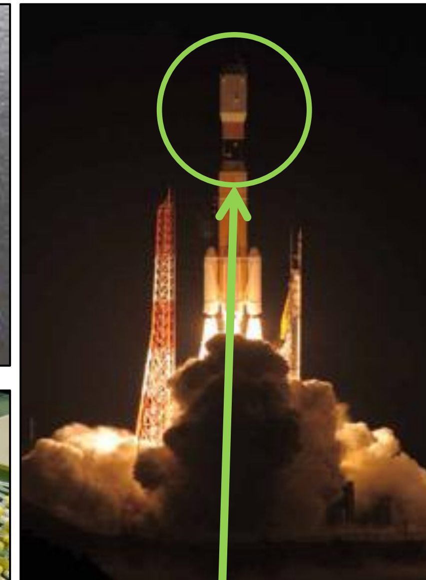

HTV (Kounotori) 5

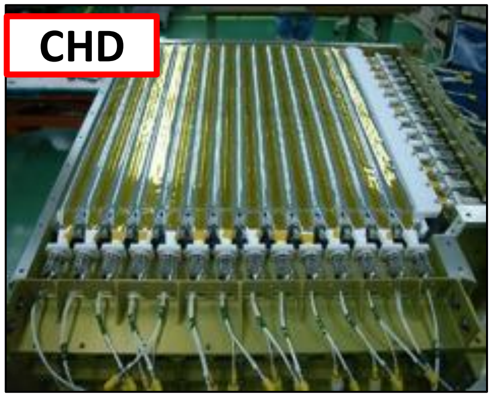

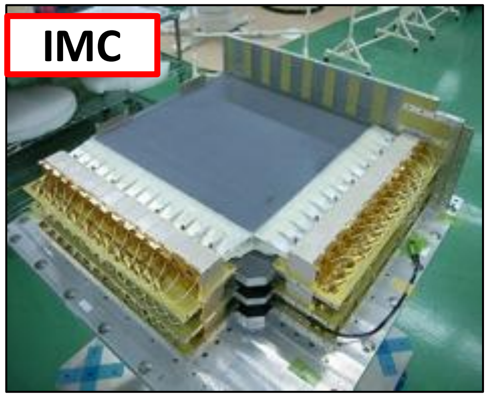

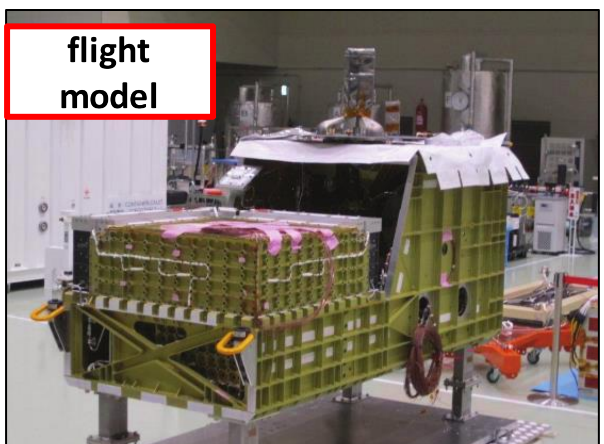

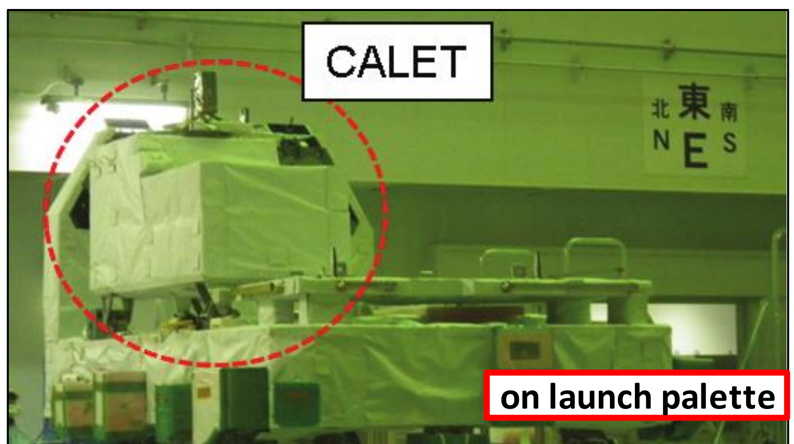

Calibration of the TASC on ground

Asaoka et al. 2017, Astropart. Phys. 91, 1—10

UV laser injection to calibrate adjacent gain ranges

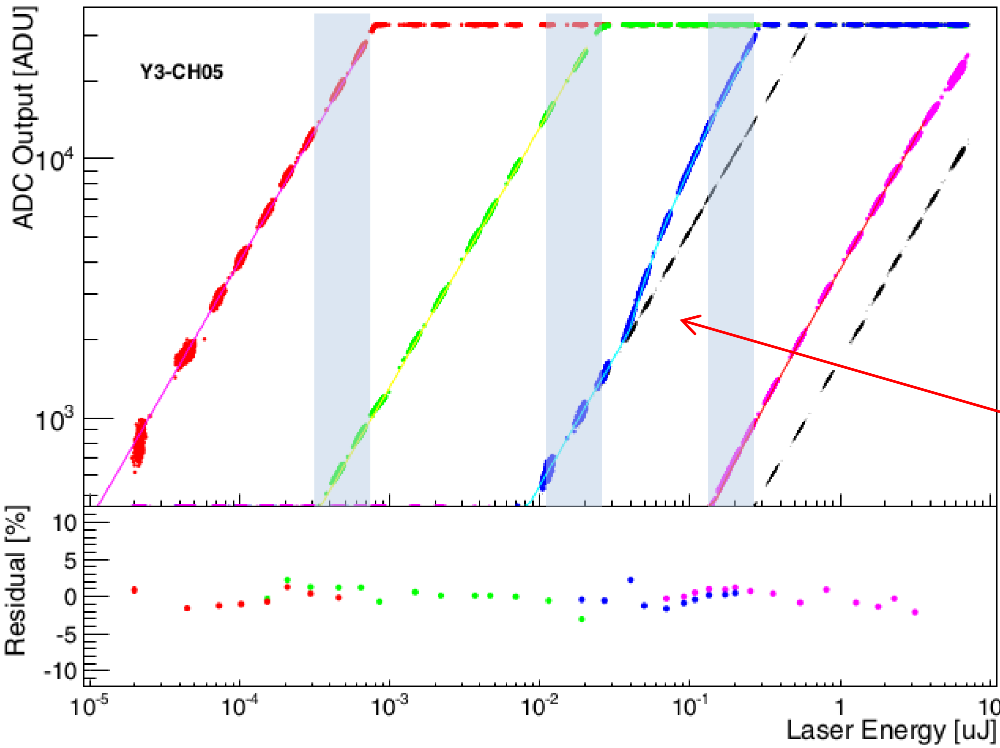

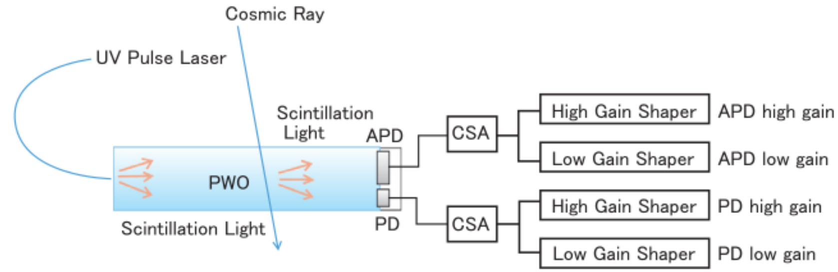

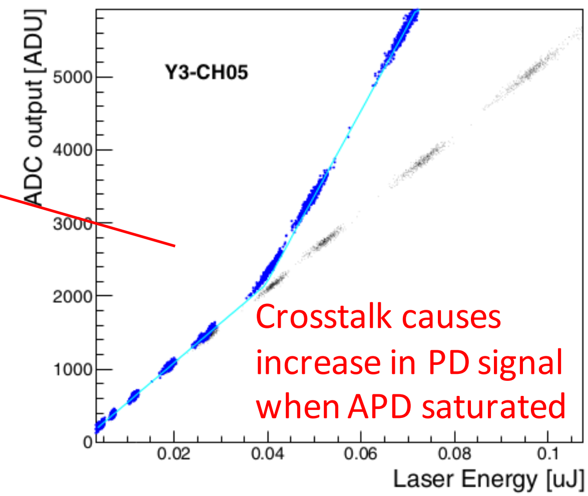

Analyzed on orbit to characterize changes from new environment:

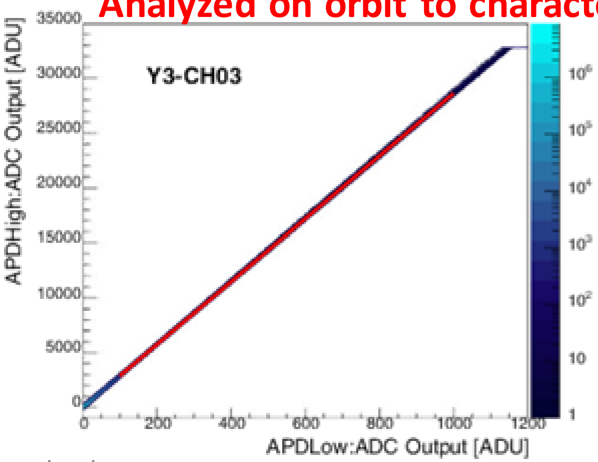

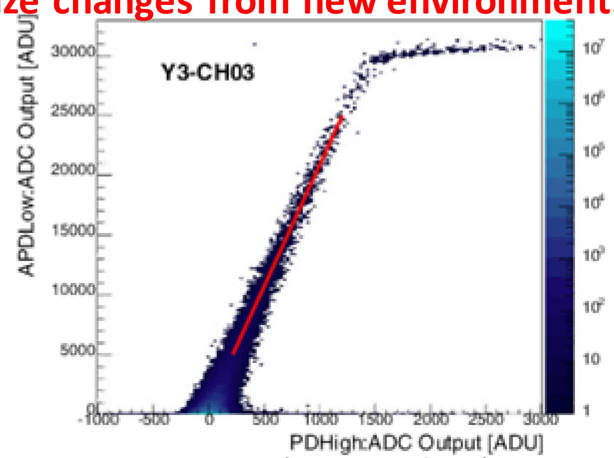

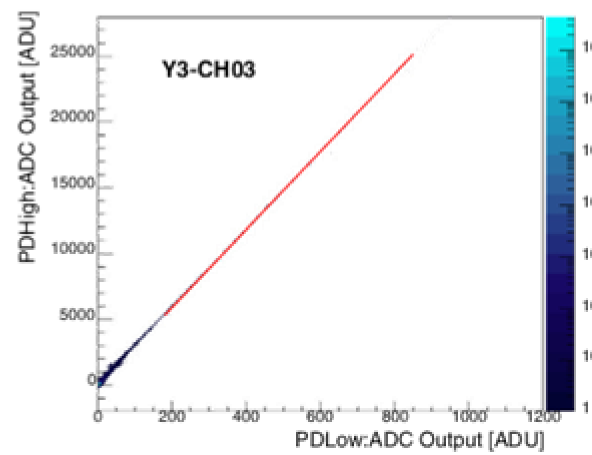

Calibration of the TASC on-orbit

Asaoka et al. 2017, Astropart. Phys. 91, 1—10

Proton and Helium MIP peaks compared with MC

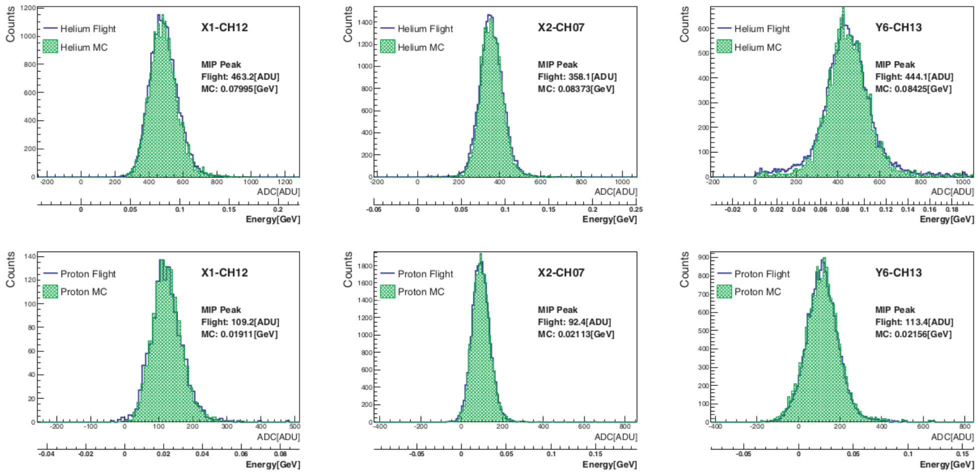

Positional dependence

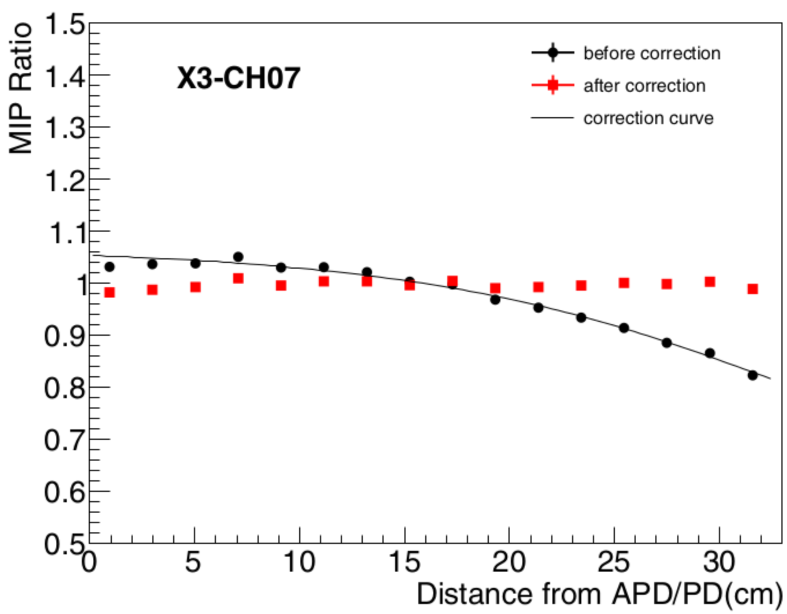

Temperature dependence

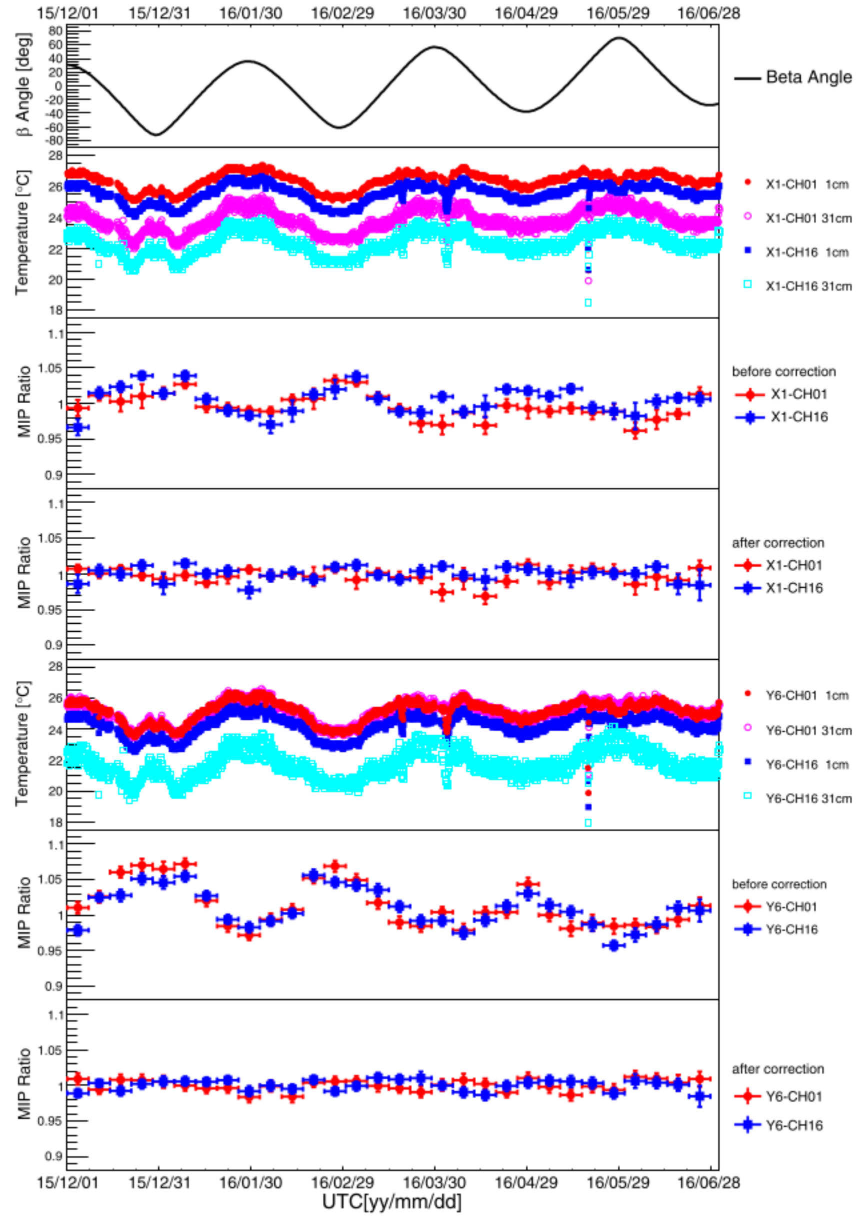

& other time dependent corrections

Operational modes

Asaoka et al. 2018, Astropart. Phys. 100, 29—37

Layers used to generate trigger primitives

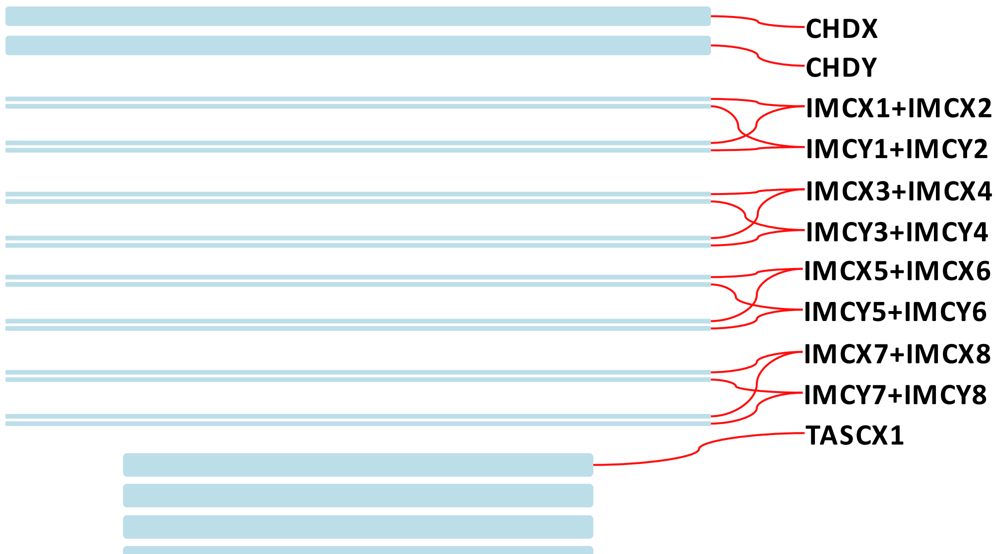

Obs. Mode	CHD X Y [MIP]	IMC X1 Y1 [MIP]	IMC X2 Y2 [MIP]	IMC X3 Y3 [MIP]	IMC X4 Y4 [MIP]	TASC X1 [MIP]
HE	-	-	-	-	16	76
	-	-	-	-	16	
LE-*e*	0.3	0.3	0.3	0.3	2.5	7
	0.3	0.3	0.3	0.3	2.5	
LE-*γ*	-	-	-	-	2.5	7
	-	-	-	-	2.5	
S-*p*	0.3	0.3	0.3	0.3	0.3	0.3
	0.3	0.3	0.3	0.3	0.3	
S-He	0.3	2.0	2.0	2.0	2.0	2.0
	0.3	2.0	2.0	2.0	2.0	
UH	100	40	40	-	-	-
	100	40	40	-	-	

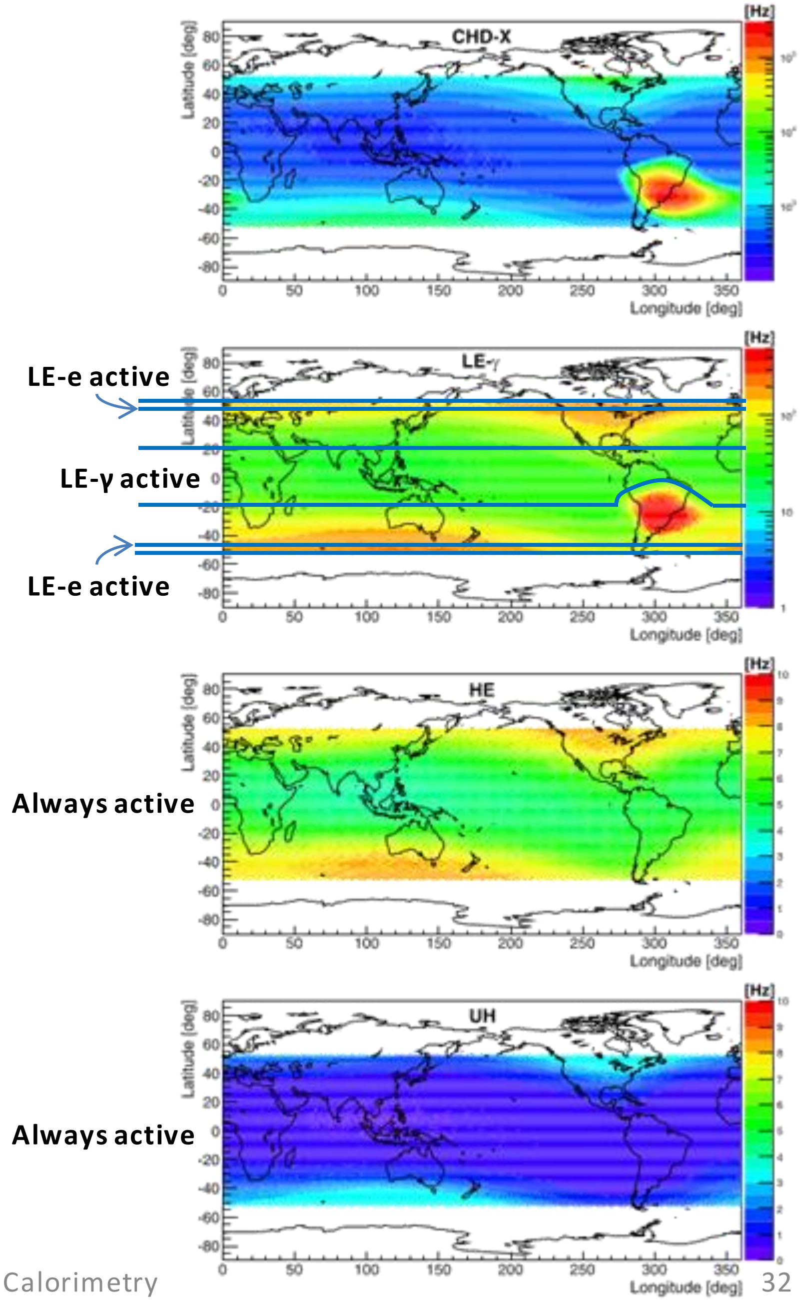

Event trigger statistics

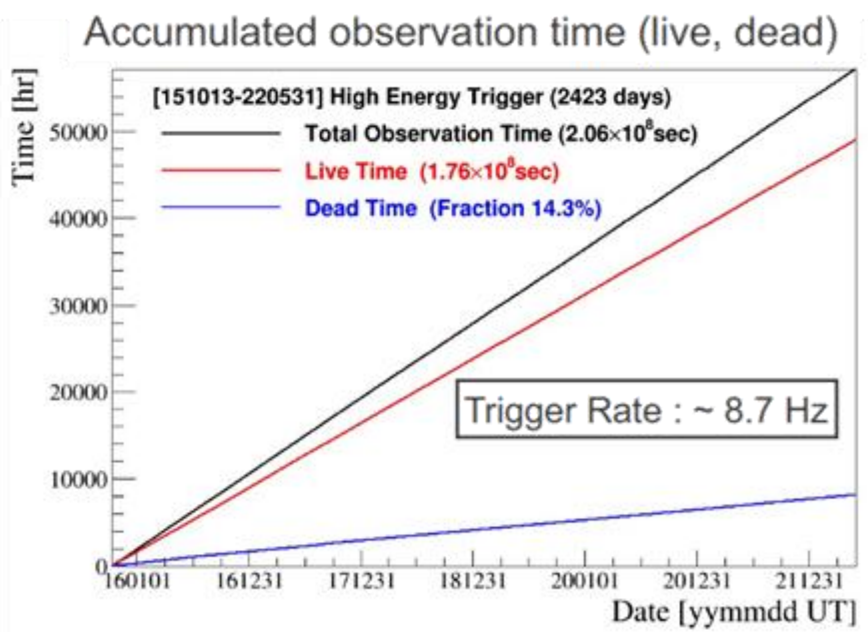

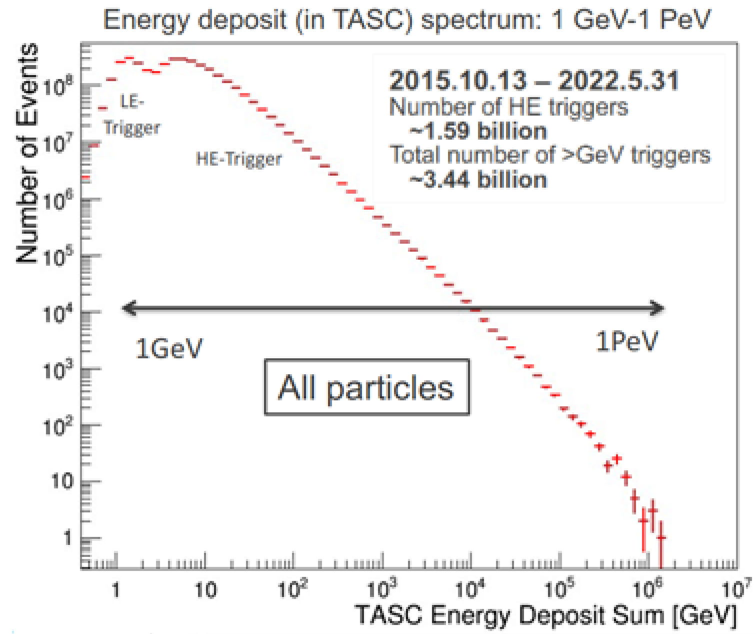

High-energy trigger (> 10 GeV) statistics:

- Operational time > **2,423 days**(*)
  (*) as of May 31, 2022
- Live time fraction **> 85%**
- Exposure of HE trigger
  ~211 m^2 sr day
- HE-gamma point source exposure
  ~4.1 m^2 day (for Crab, Geminga)

Electron selection requirements (E < 500 GeV)

Trigger selection

- Online trigger satisfied
- Offline trigger satisfied

Track quality cuts

- NpX > 4= && NpY >= 4
- |NpX – NpY| ≤ 1
- TASC consistency

Electron selection cuts

- CHD and IMC charge selection
- Shower development threshold
- Electron likelihood
- IMC concentration
- Two-parameter K-cut

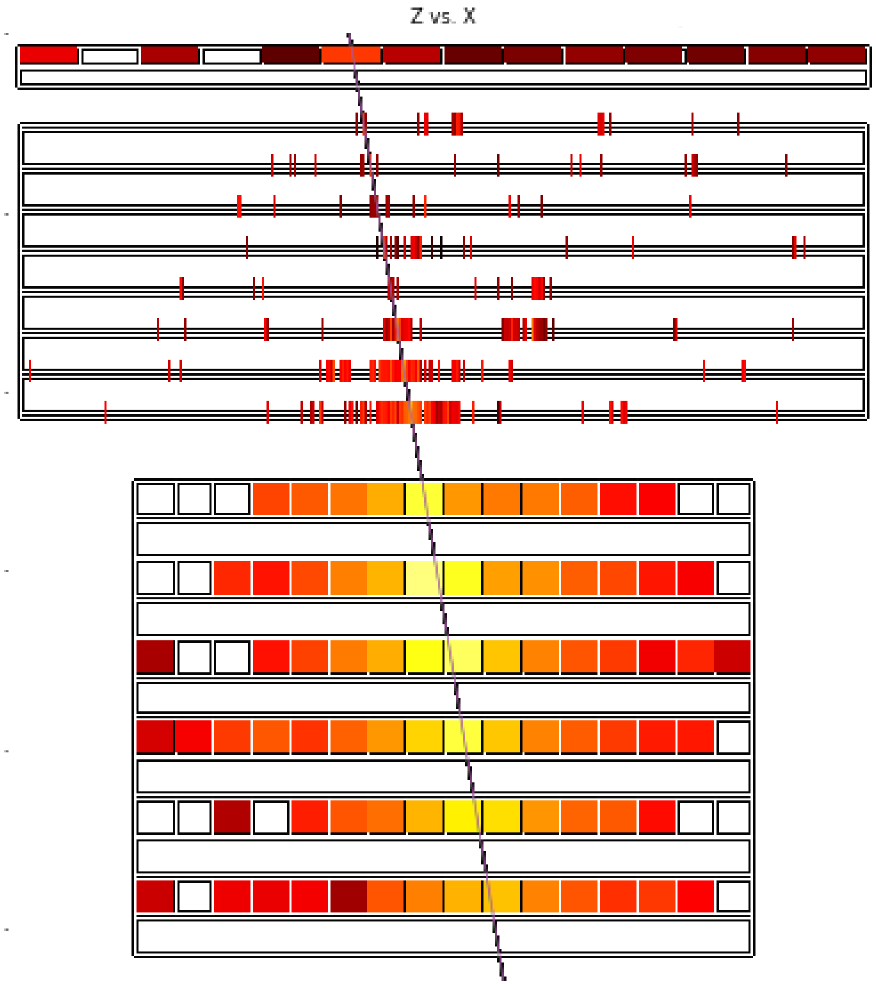

Electron selection requirements (E < 500 GeV)

Trigger selection

- **Online trigger satisfied**
- **Offline trigger satisfied**

Track quality cuts

- NpX > 4= && NpY >= 4
- |NpX – NpY| ≤ 1
- TASC consistency

Electron selection cuts

- CHD and IMC charge selection
- Shower development threshold
- Electron likelihood
- IMC concentration
- Two-parameter K-cut

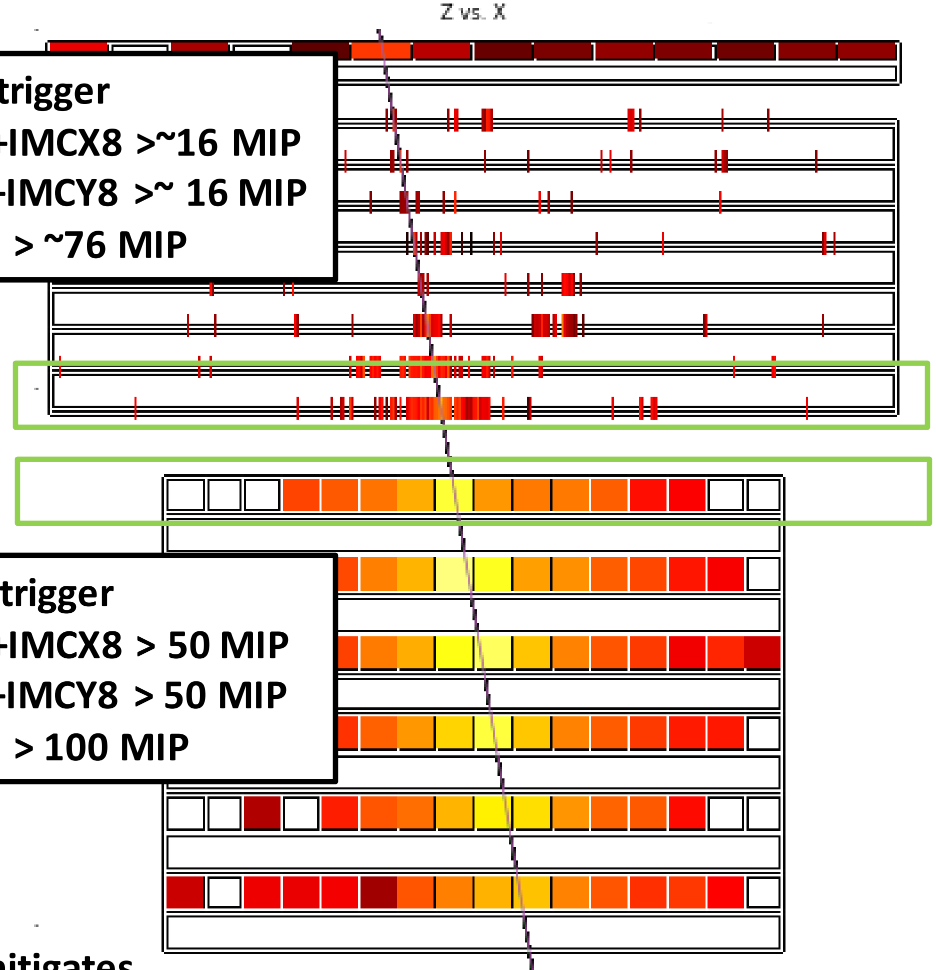

Online HE trigger

- IMCX7+IMCX8 >~16 MIP
- IMCY7+IMCY8 >~ 16 MIP
- TASCX1 > ~76 MIP

Offline HE trigger

- IMCX7+IMCX8 > 50 MIP
- IMCY7+IMCY8 > 50 MIP
- TASCX1 > 100 MIP

Offline trigger mitigates edge effects, i.e. small temperature-dependent threshold shifts

Electron selection requirements (E < 500 GeV)

Trigger selection

- Online trigger satisfied
- Offline trigger satisfied

Track quality cuts

- **NpX > 4 = && NpY >= 4**
- **|NpX – NpY| ≤ 1**
- **TASC consistency**

Electron selection cuts

- CHD and IMC charge selection
- Shower development thre
- Electron likelihood
- IMC concentration
- Two-parameter K-cut

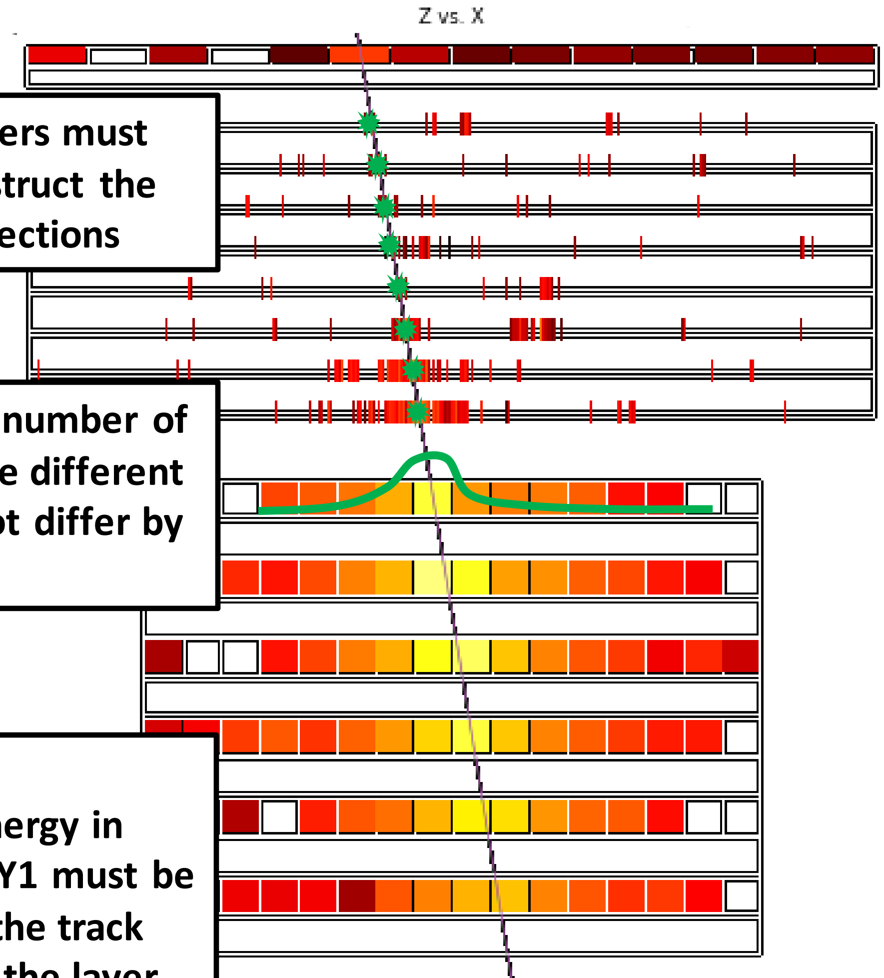

At least 4 IMC layers must be used to reconstruct the track in both projections

The difference in number of layers used for the different projections cannot differ by more than one

TASC consistency
- The center of energy in TASCX1 and TASCY1 must be within 2.5 cm of the track intersection with the layer

Electron selection requirements (E < 500 GeV)

Trigger selection
- Online trigger satisfied
- Offline trigger satisfied

Track quality cuts
- NpX > 4= && NpY >= 4
- |NpX – NpY| ≤ 1
- TASC consistency

Electron selection cuts
- **CHD and IMC charge selection**
- Shower development threshold
- Electron likelihood
- IMC concentration
- Two-parameter K-cut

The signal in the CHD and/or incident layer of the IMC must be consistent with a singly-charged primary, including tolerance for noise and backscatter

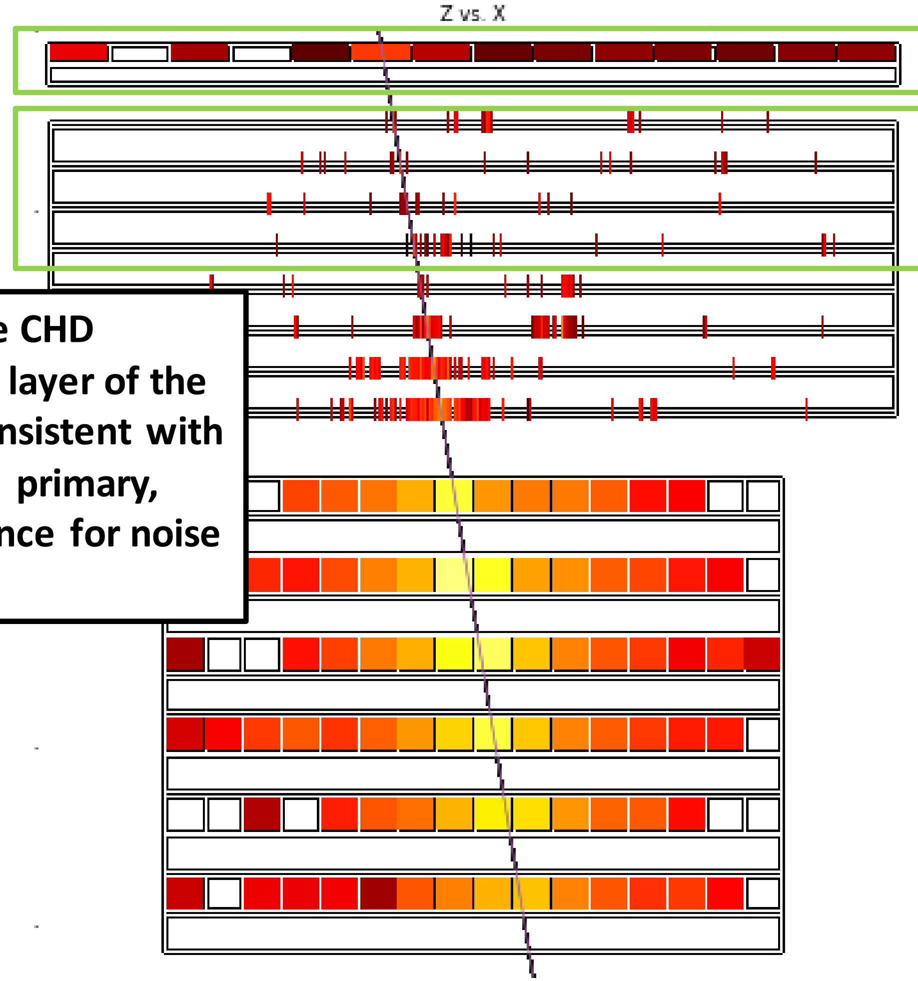

Electron selection requirements (E < 500 GeV)

Trigger selection

- Online trigger satisfied
- Offline trigger satisfied

Track quality cuts

- NpX > 4= && NpY >= 4
- |NpX – NpY| ≤ 1
- TASC consistency

Electron selection cuts

- CHD and IMC charge selection
- **Shower development threshold**
- Electron likelihood
- IMC concentration
- Two-parameter K-cut

The signal in the bottom of the IMC must be consistent with the shower having started

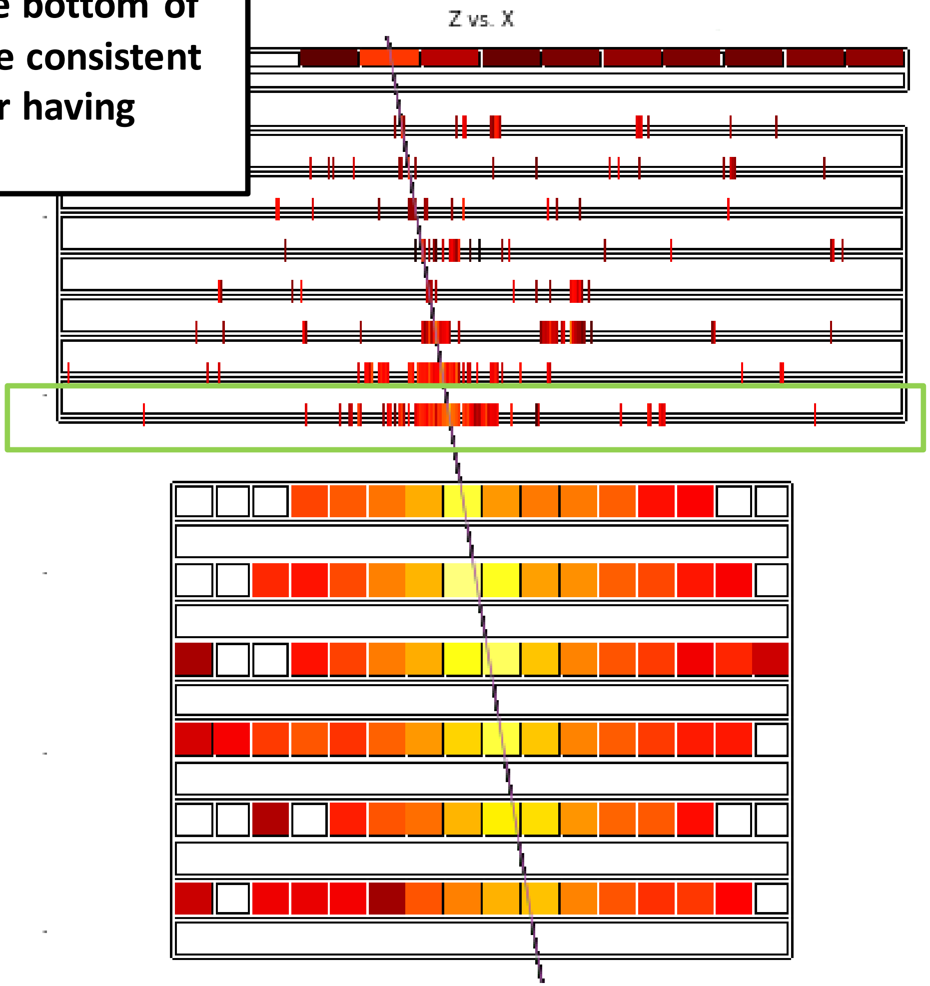

Electron selection requirements (E < 500 GeV)

Trigger selection

- Online trigger satisfied
- Offline trigger satisfied

Track quality cuts

- NpX > 4= && NpY >= 4
- |NpX – NpY| ≤ 1
- TASC consistency

Electron selection cuts

- CHD and IMC charge selection
- Shower development thre
- **Electron likelihood**
- IMC concentration
- Two-parameter K-cut

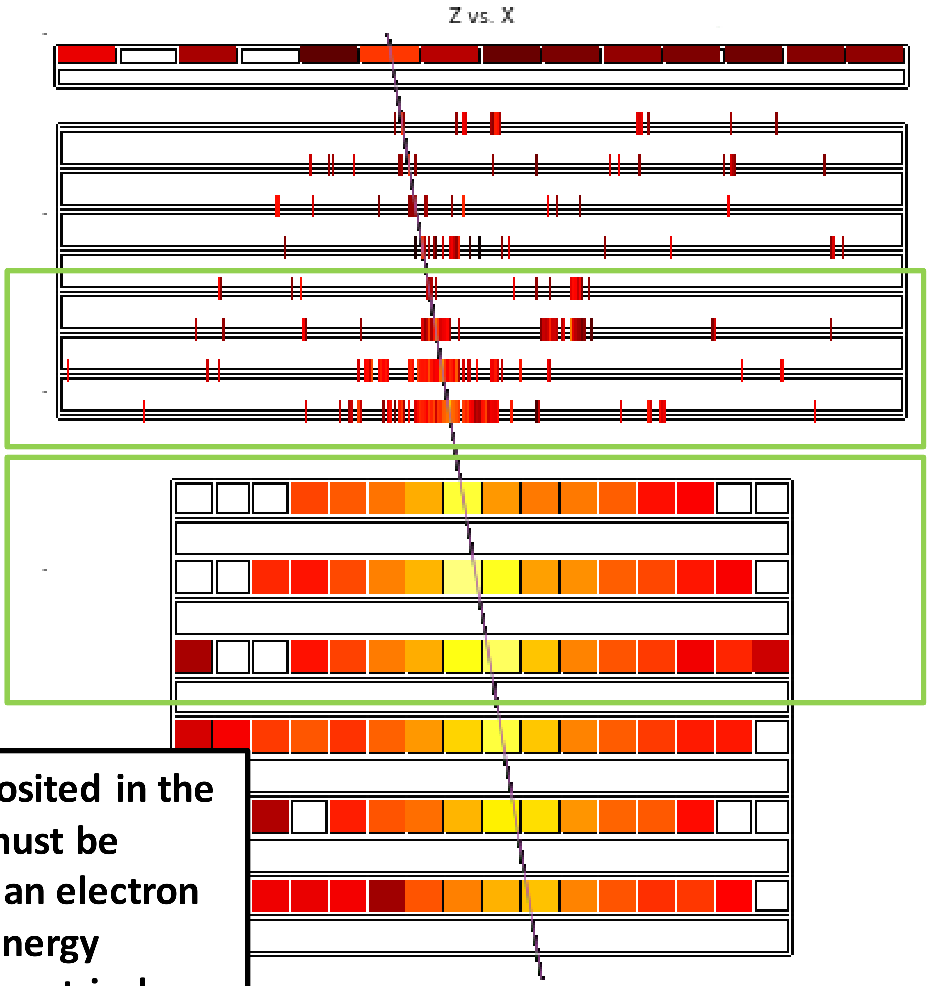

The energy deposited in the IMC and TASC must be consistent with an electron with this total energy deposit and geometrical acceptance

Electron selection requirements (E < 500 GeV)

Trigger selection

- Online trigger satisfied
- Offline trigger satisfied

Track quality cuts

- NpX > 4= && NpY >= 4
- |NpX – NpY| ≤ 1
- TASC consistency

Electron selection cuts

- CHD and IMC charge selection
- Shower development threshold
- Electron likelihood
- **IMC concentration**
- Two-parameter K-cut

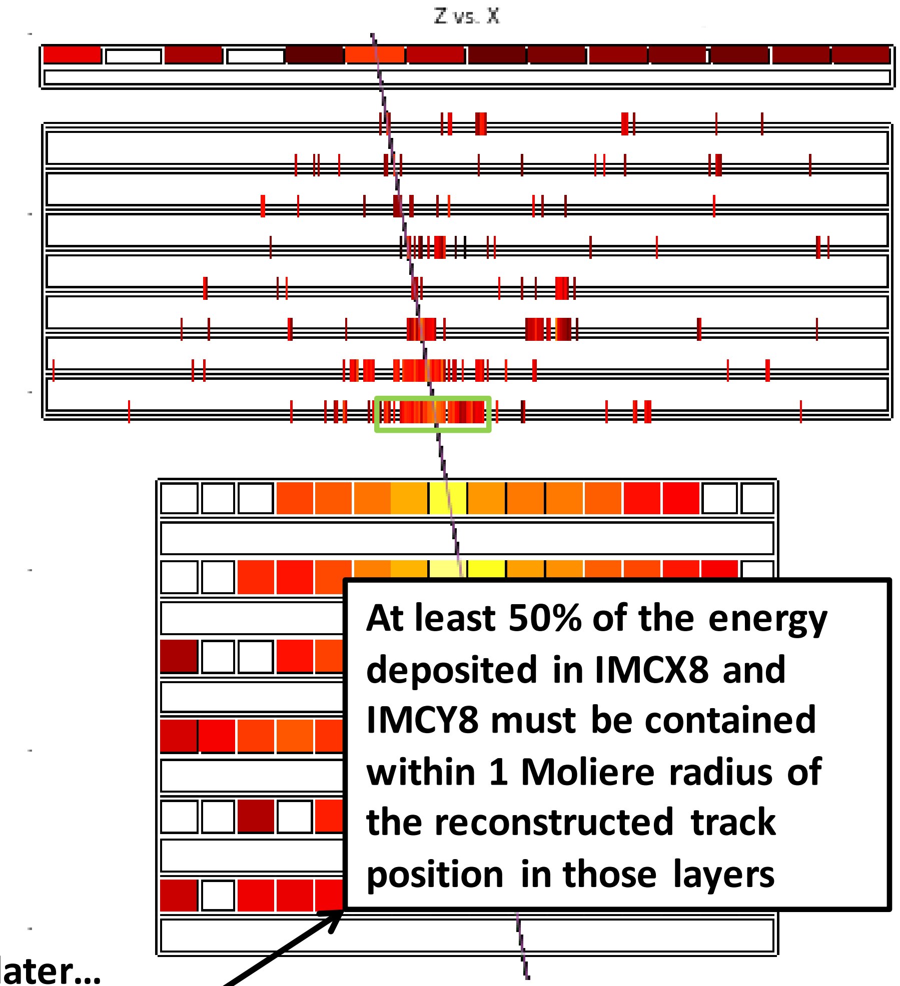

At least 50% of the energy deposited in IMCX8 and IMCY8 must be contained within 1 Moliere radius of the reconstructed track position in those layers

To be discussed later…
Hadronic showers have a less tightly-contained energy deposit profile

Electron selection requirements (E < 500 GeV)

Trigger selection

- Online trigger satisfied
- Offline trigger satisfied

Track quality cuts

- NpX > 4= && NpY >= 4
- |NpX – NpY| ≤ 1
- TASC consistency

Electron selection cuts

- CHD and IMC charge selection
- Shower development threshold
- Electron likelihood
- IMC concentration
- **Two-parameter K-cut**

Two parameters describe the shower topology in the TASC:

- **R_E: the lateral width of the shower profile in TASCX1 based on energy deposits >3 MIP**
- **F_E: the fraction of energy deposited in the bottom layer of the TASC**

These two parameters are combined to make K:

$$K = 0.5\, R_E + \log_{10} F_E$$

As before, expected to be larger for hadrons since shower more laterally distributed

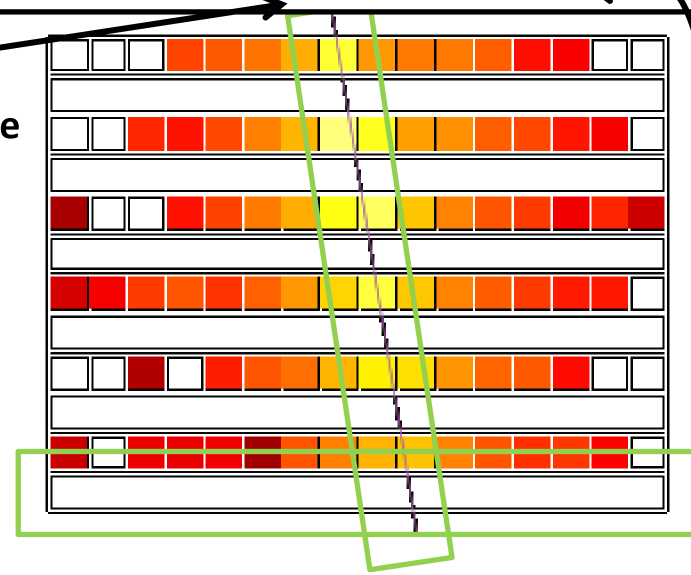

Larger for hadronic primaries as well due to more penetrating secondaries

Electron selection requirements (E > 500 GeV)

Trigger selection

- Online trigger satisfied
- Offline trigger satisfied

Track quality cuts

- NpX > 4= && NpY >= 4
- |NpX – NpY| ≤ 1
- TASC consistency

Electron selection cuts

- CHD and IMC charge selection
- Shower development threshold
- Electron likelihood
- IMC concentration
- **BDT cut**

Due to increasing proton contamination, a machine learning algorithm based on Boosted Decision Trees (BDT) is used to separate hadrons from electrons instead of the K-cut

BDT trained on physically-motivated parameters in different energy ranges:

1. The shower width in TASCX1, R_E
2. The fraction of energy in TASCY6, F_E
3. The IMCY8 shower concentration
4. Parameters for the TASC shower fit:
    - Shower maximum (α/b)
    - Attenuation constant (b)
    - 5% shower depth ($T_{5\%}$)
    - Goodness of fit (χ^2_{TASC})
5. Parameters for the IMC shower fit:
    - Exponential fit constant (p0)
    - Exponential fit slope (p1)
    - Goodness of fit (χ^2_{IMC})

Above 500 GeV, all of these except (3) are used

Selection efficiency for electrons and residual protons

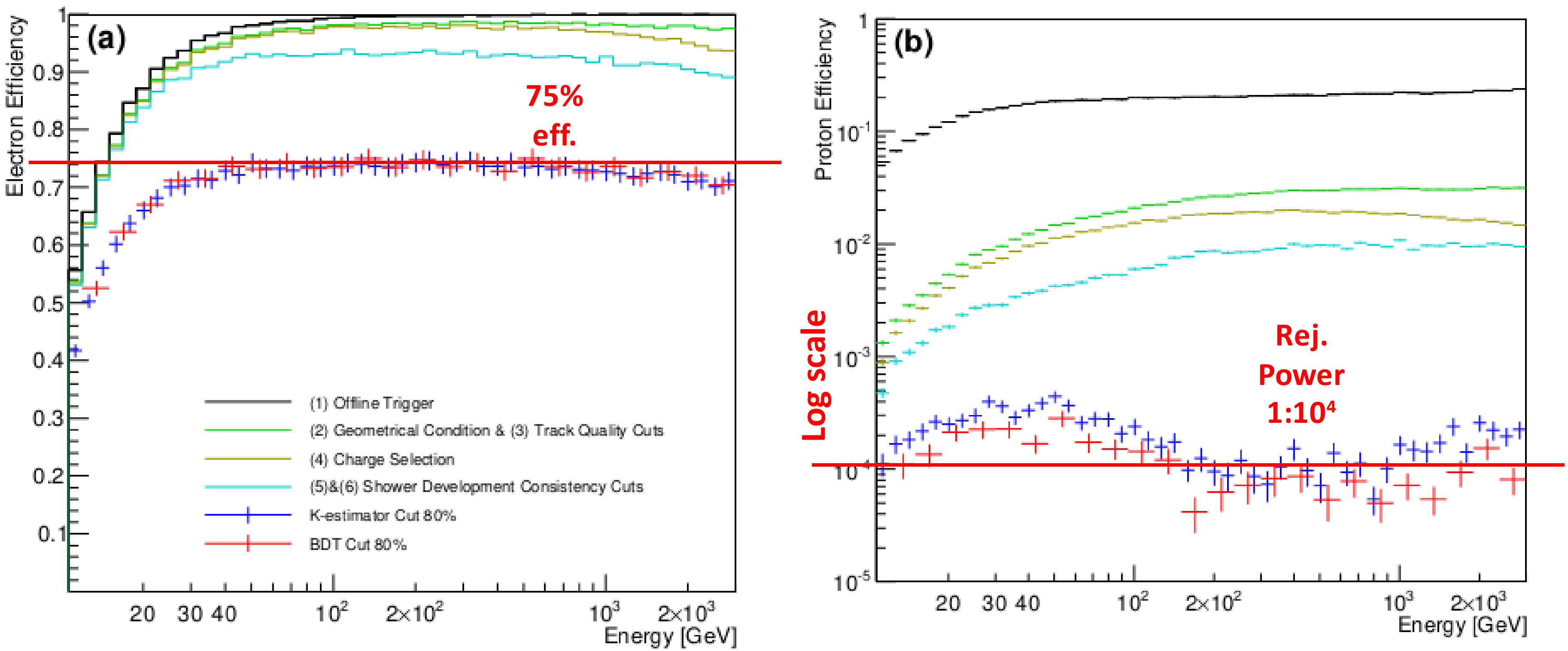

FIG. 3. (a) Electron efficiency as a function of energy for each important selection step. (b) Same for protons. Black, green, yellow, blue and red histograms show the efficiency after (1) offline trigger, (2) geometrical condition with (3) track quality cuts, (4) charge selection, and (5)&(6) shower development consistency cuts, K-estimator cut with 80% efficiency, BDT cut with 80% efficiency, respectively.

Adriani et al. 2017
PRL 119, 181101

Electron energy resolution

Asaoka et al. 2017, Astropart. Phys. 91, 1—10

Table 1
Summary of the error budget in the energy calibration.

MIP	Energy conversion	2.6%
Peak fitting of MC and flight data		0.6%
Fitting range dependence		0.6%[a]
Position dependence		1.8%
Temperature dependence		1.0%
Rigidity cutoff dependence		1.0%[a]
Systematic uncertainty estimated from p/He consistency		1.0%
UV Laser	Linearity	1.4~ 2.5%
Fit error		
APD high gain		1.4%
APD low gain		1.5%
PD high gain		2.5%
PD low gain		2.2%
Gain Ratio	Gain range connection	1.6~ 2.1%
Fit error		
APD-high to APD-low gain		0.1%
APD-low to PD-high gain		0.7%
PD high to PD low gain		0.1%
Slope extrapolation		
APD-high to APD-low gain		1.6%
APD-low to PD-high gain		2.0%[a]
PD high to PD low gain		1.8%
Sampling Bias		0.5%[b]

[a] also considered as systematic error on energy scale
[b] energy-scale systematic error only

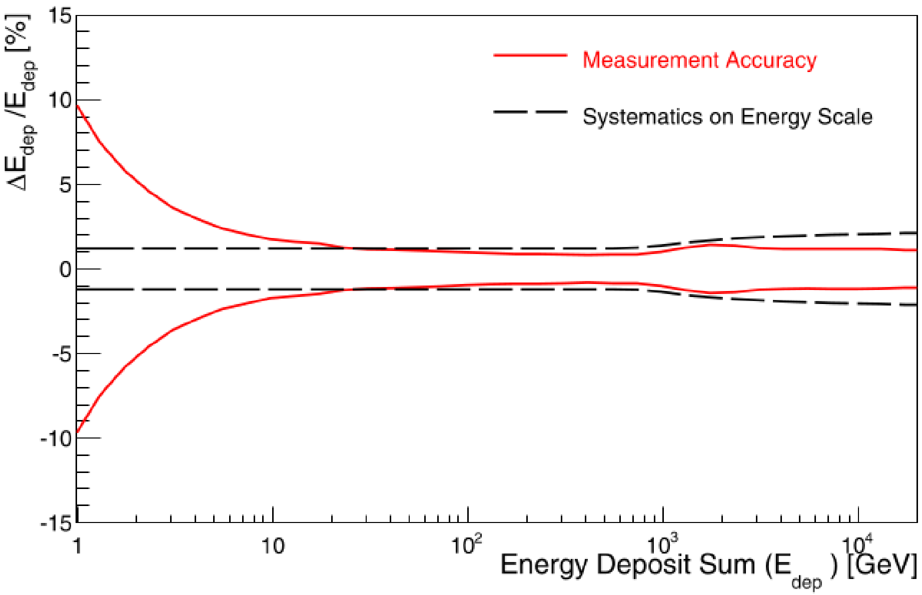

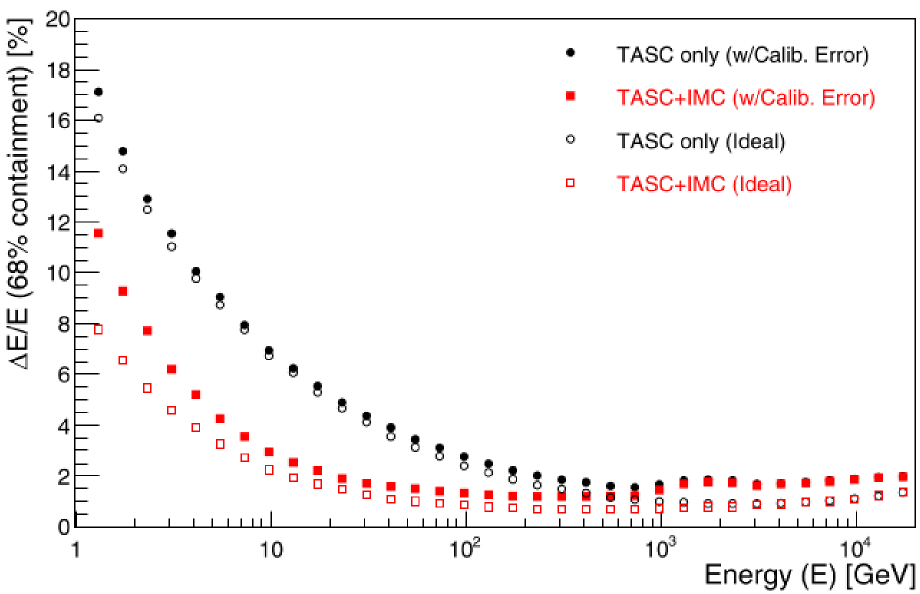

Absolute energy scale calibration on-orbit

The Earth's magnetic field creates a low-rigidity cutoff where charged particles *cannot* reach the detector – the cutoff varies as a function of position in the orbit and direction

M. Ackermann et al. / Astroparticle Physics 35 (2012) 346–353

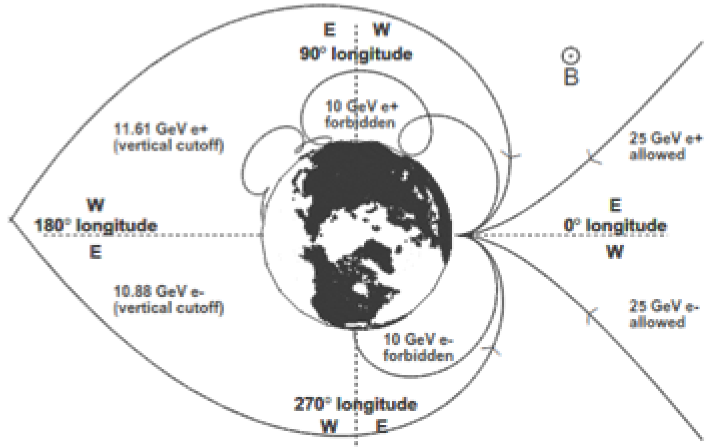

Using a model for the magnetic field and ray-tracing code to determine the cutoffs, a correcting factor for the energy of electrons can be derived for individual experiments

Example figures from Fermi-LAT (AP 35 346 (2012))

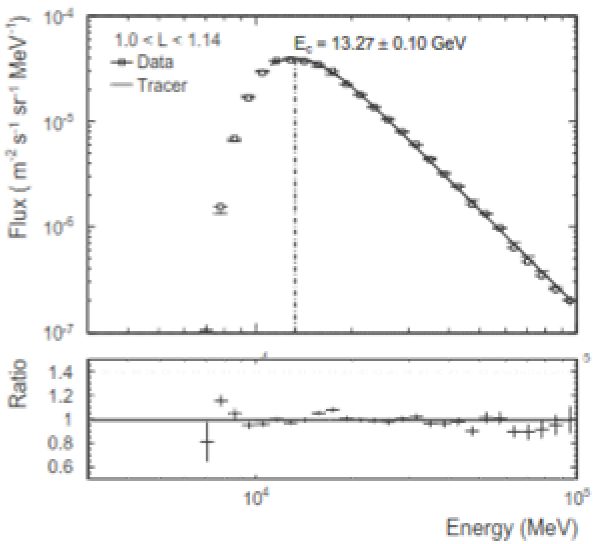

Fig. 5. Energy spectrum of data and tracer for the McIlwain *L* interval 1.0 < *L* < 1.14. The black line is a fit to the data using Eq. (1) and the resulting cutoff energy has a value of 13.27 ± 0.10 GeV, and is indicated by the dot dashed line in the figure. The lower panel depicts the ratio of the two spectra.

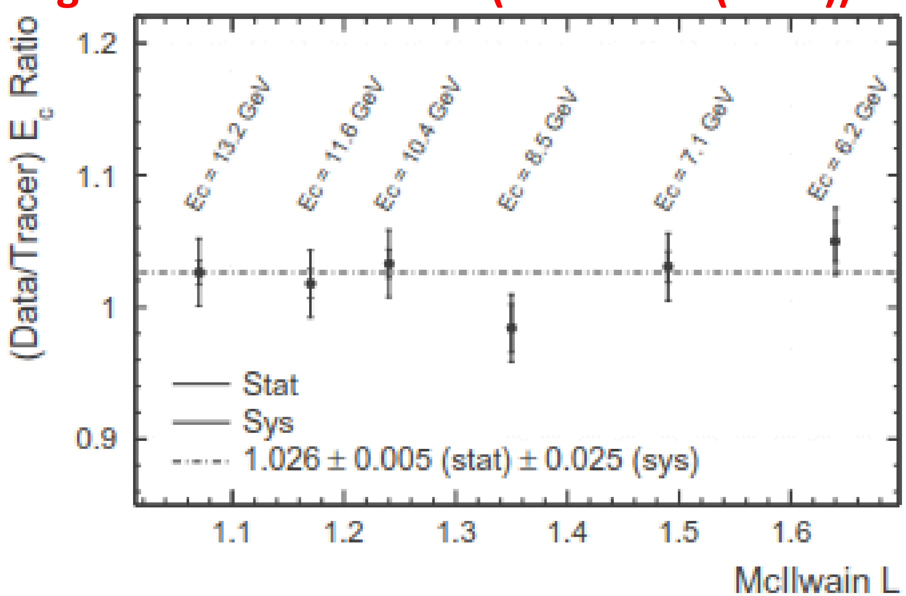

Correction factor for CALET measured to be ~3.5%

Other space-borne calorimeters

Dark Matter Particle Explorer (DAMPE)

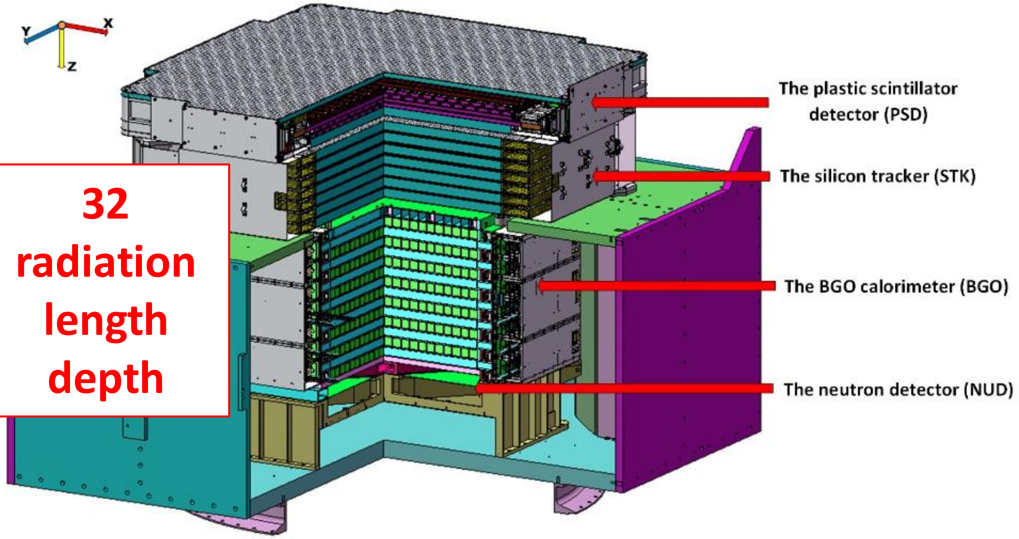

32 radiation length depth

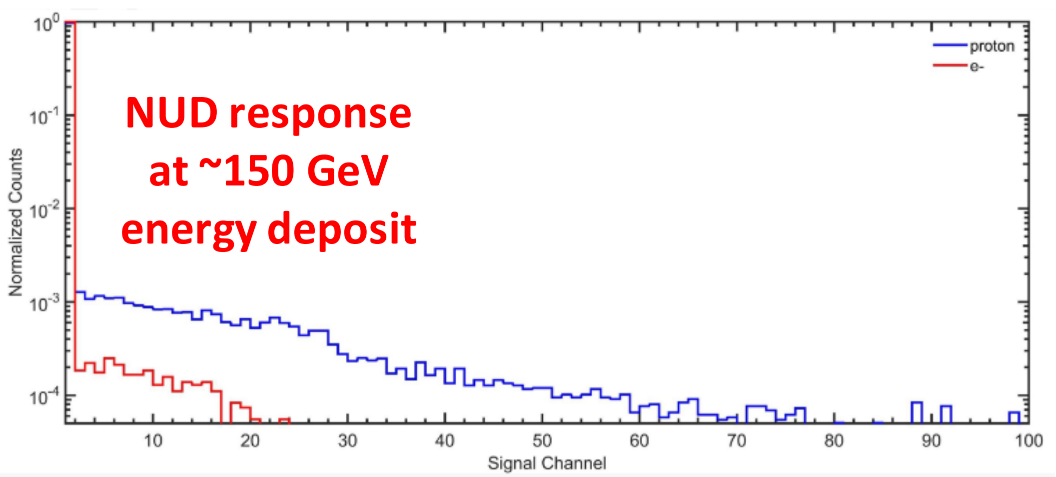

NUD response at ~150 GeV energy deposit

Astropart. Phys. 95, 6 (2017)

Fermi Large Area Telescope (LAT)

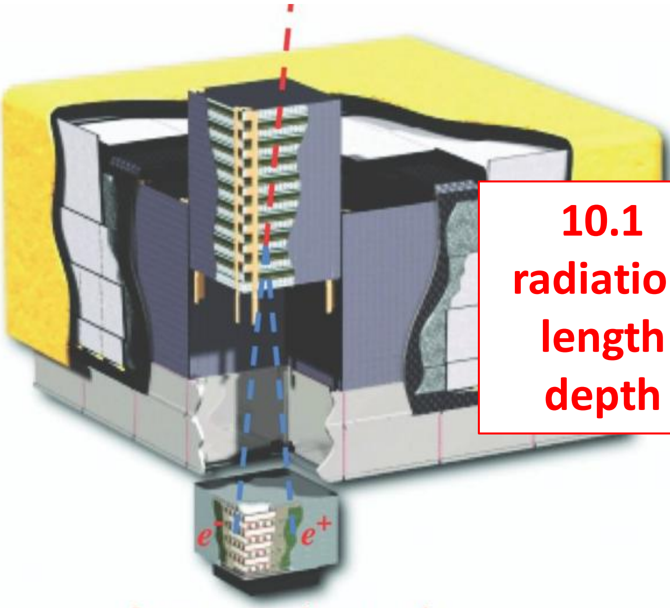

10.1 radiation length depth

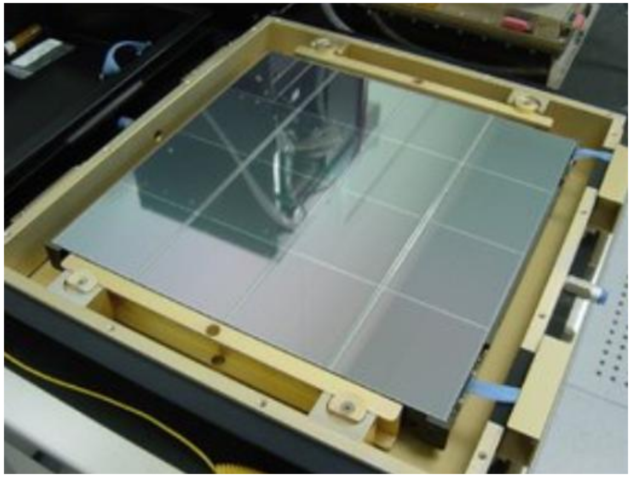

Astrophys. J. 697, 1071 (2009)

Electron energy spectrum

PHYSICAL REVIEW LETTERS **120,** 261102 (2018)

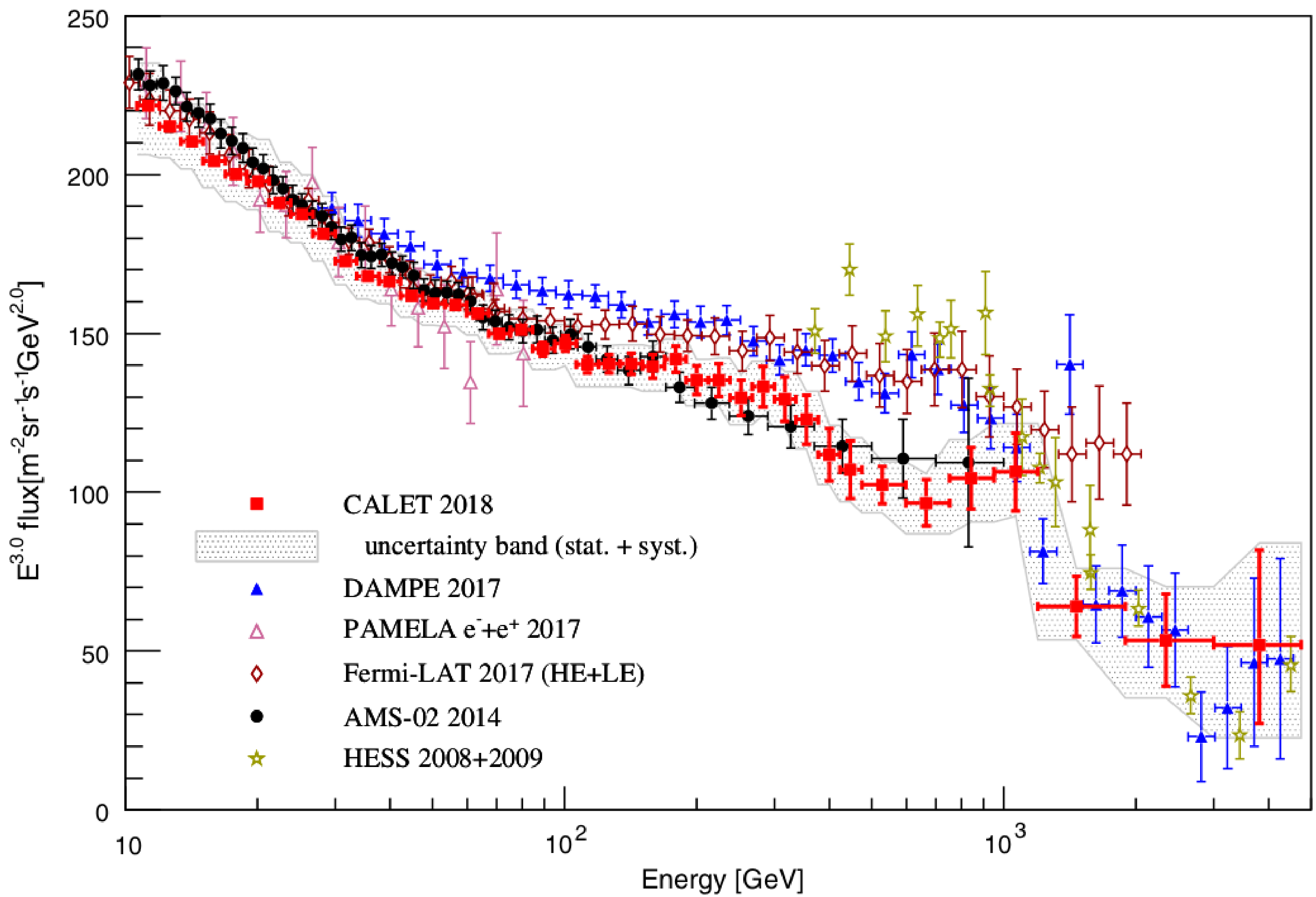

Electron energy spectrum

- CALET results consistent with AMS-02 below 1 TeV
- Two groups of measurements below ~1 TeV:
  - AMS-02 + CALET
  - Fermi-LAT + DAMPE

indicating the presence of unknown systematics

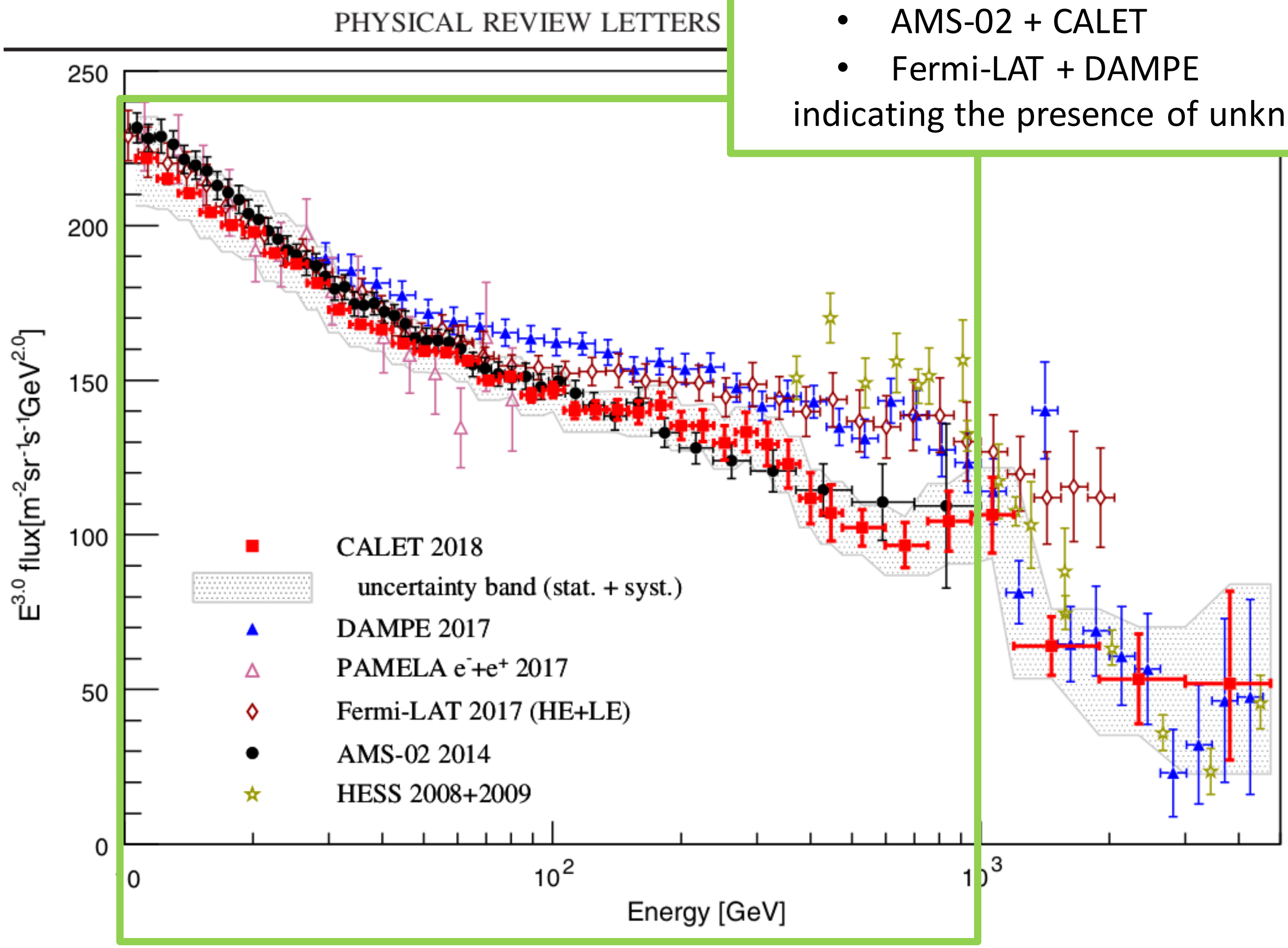

Electron energy spectrum

Many papers probing possible peak in DAMPE data- not mentioned in original publication

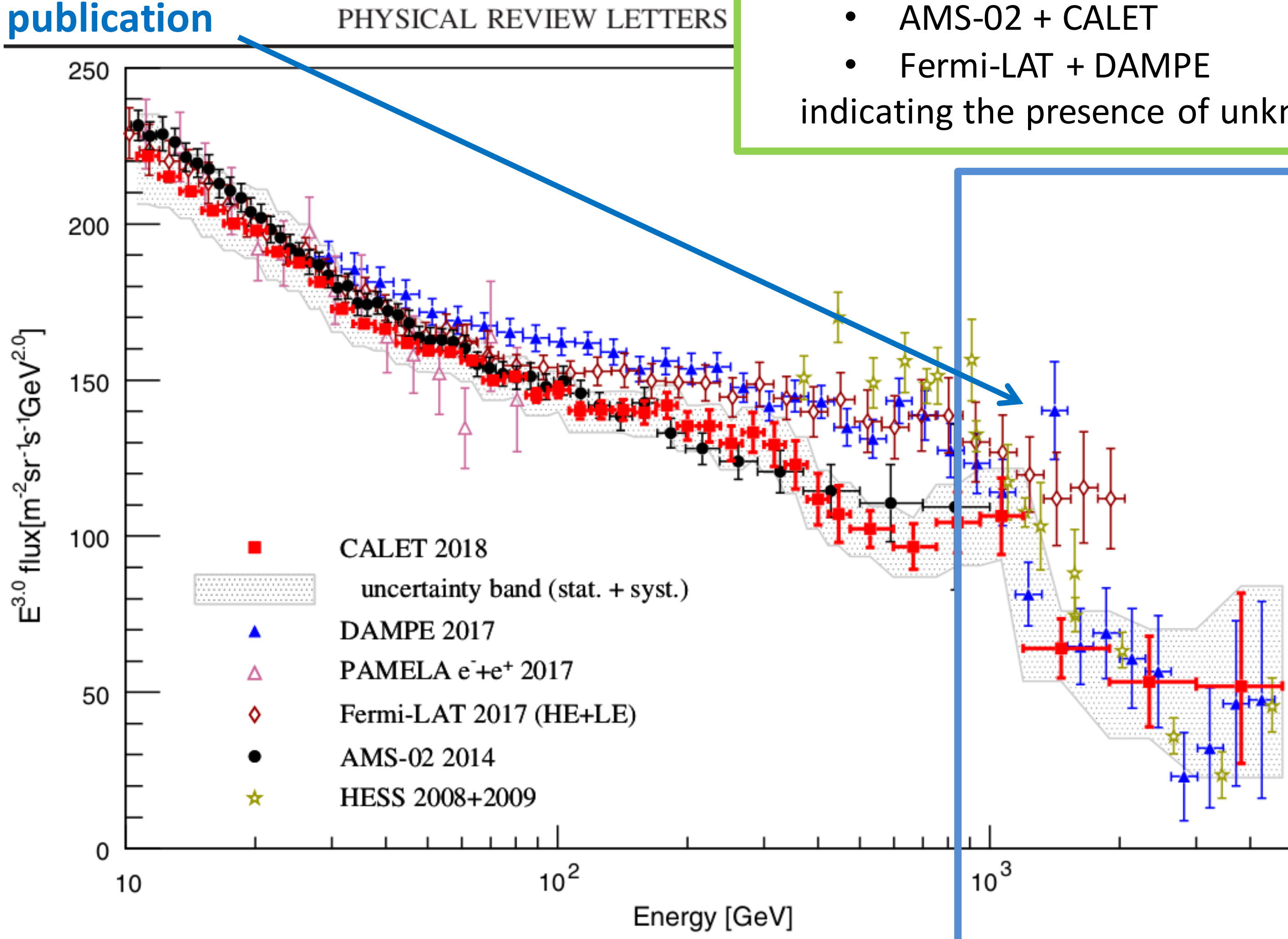

- CALET results consistent with AMS-02 below 1 TeV
- Two groups of measurements below ~1 TeV:
  - AMS-02 + CALET
  - Fermi-LAT + DAMPE

  indicating the presence of unknown systematics

- CALET observes flux suppression above 1 TeV consistent with DAMPE within errors
- No peak-like structure at 1.4 TeV in CALET measurement irrespective of binning

Electron energy spectrum

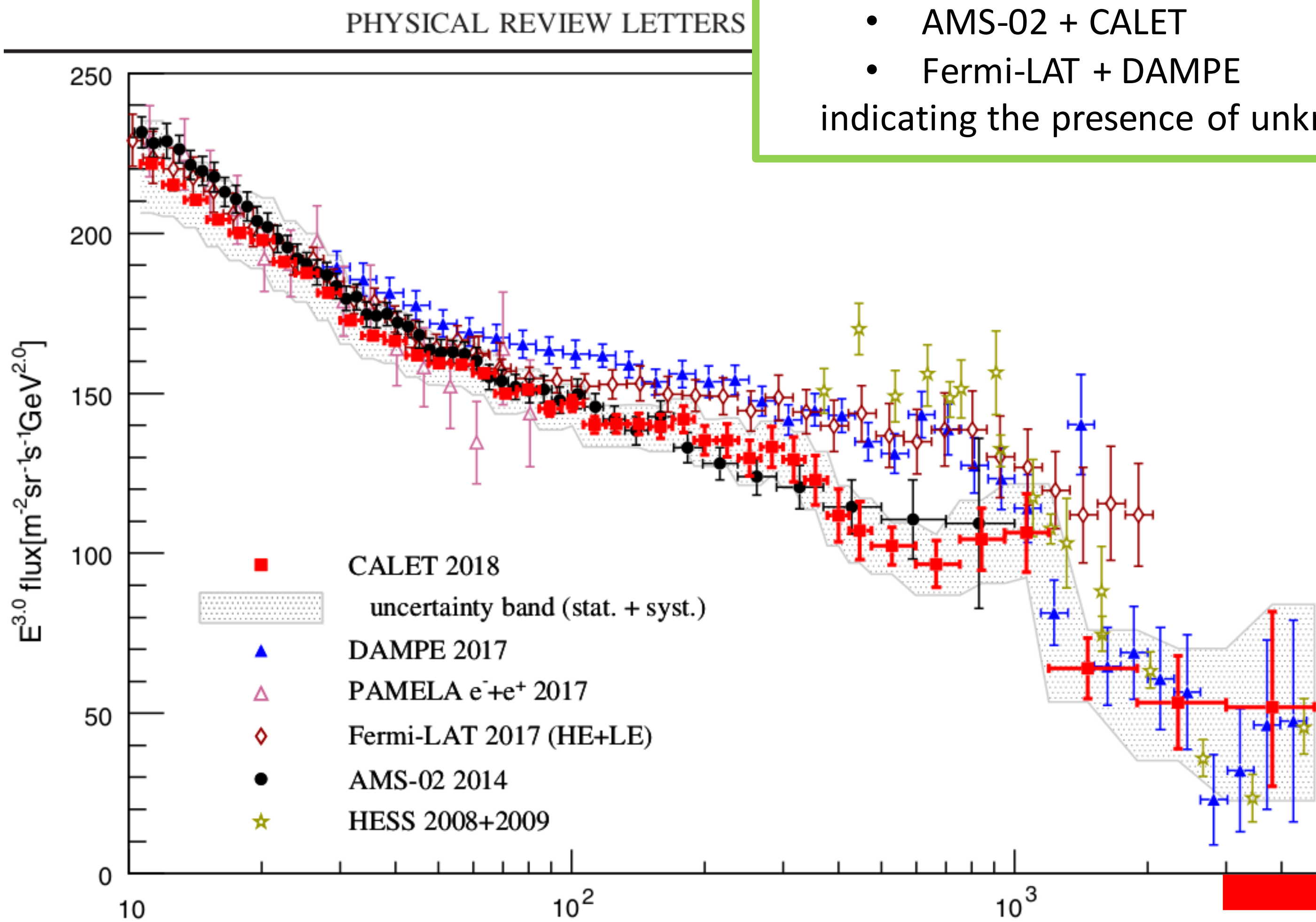

- CALET results consistent with AMS-02 below 1 TeV
- Two groups of measurements below ~1 TeV:
  - AMS-02 + CALET
  - Fermi-LAT + DAMPE

indicating the presence of unknown systematics

- CALET observes flux suppression above 1 TeV consistent with DAMPE within errors
- No peak-like structure at 1.4 TeV in CALET measurement irrespective of binning

- Features above ~few TeV would indicate nearby source
- Electron candidate events with E >~10 TeV being studied in event-by-event analysis

Systematic errors on the CALET measurement

In addition to the statistical errors in the results, it is critical to study *systematic* errors from analysis choices

i.e. energy-dependent variation in the results can be probed via variation of analysis parameters such as (**non-exhaustive**):

- Electron survival fraction of cuts such as the K-cut, BDT, or charge selection
- MC model used for calculating instrument response
- Algorithms for reconstruction of primary particle properties such as incident direction and kinetic energy
- Binning artifacts

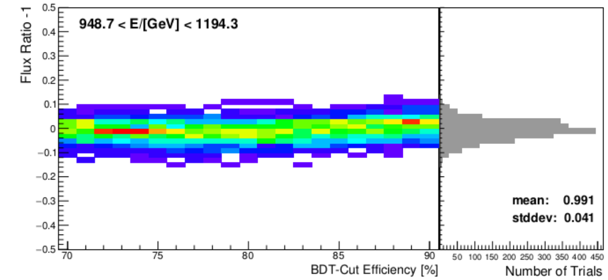

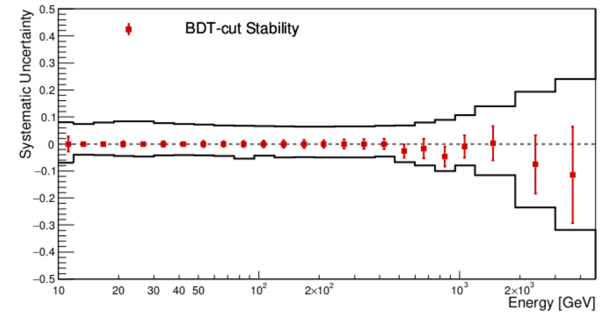

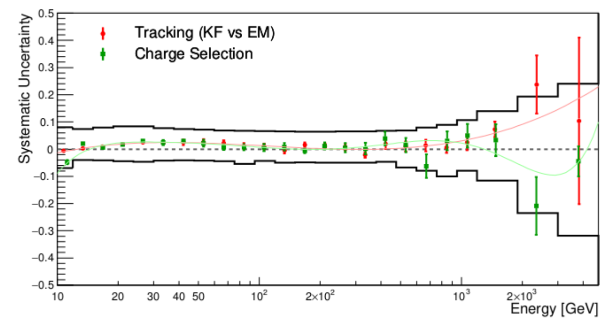

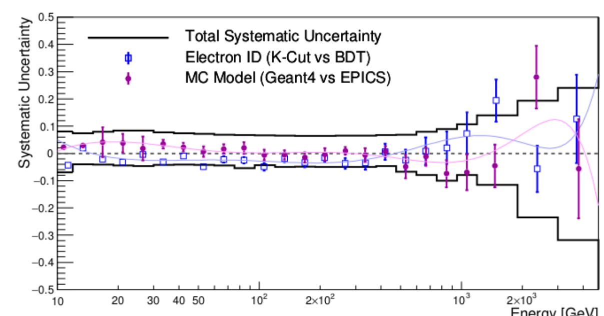

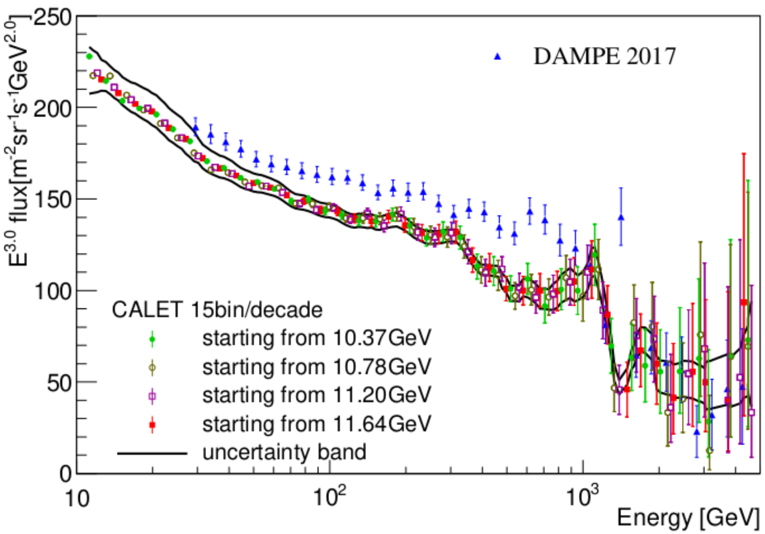

Ref: Supplemental Material for CALET PRL papers in 2017 and 2018

Electron energy spectrum (preliminary update)

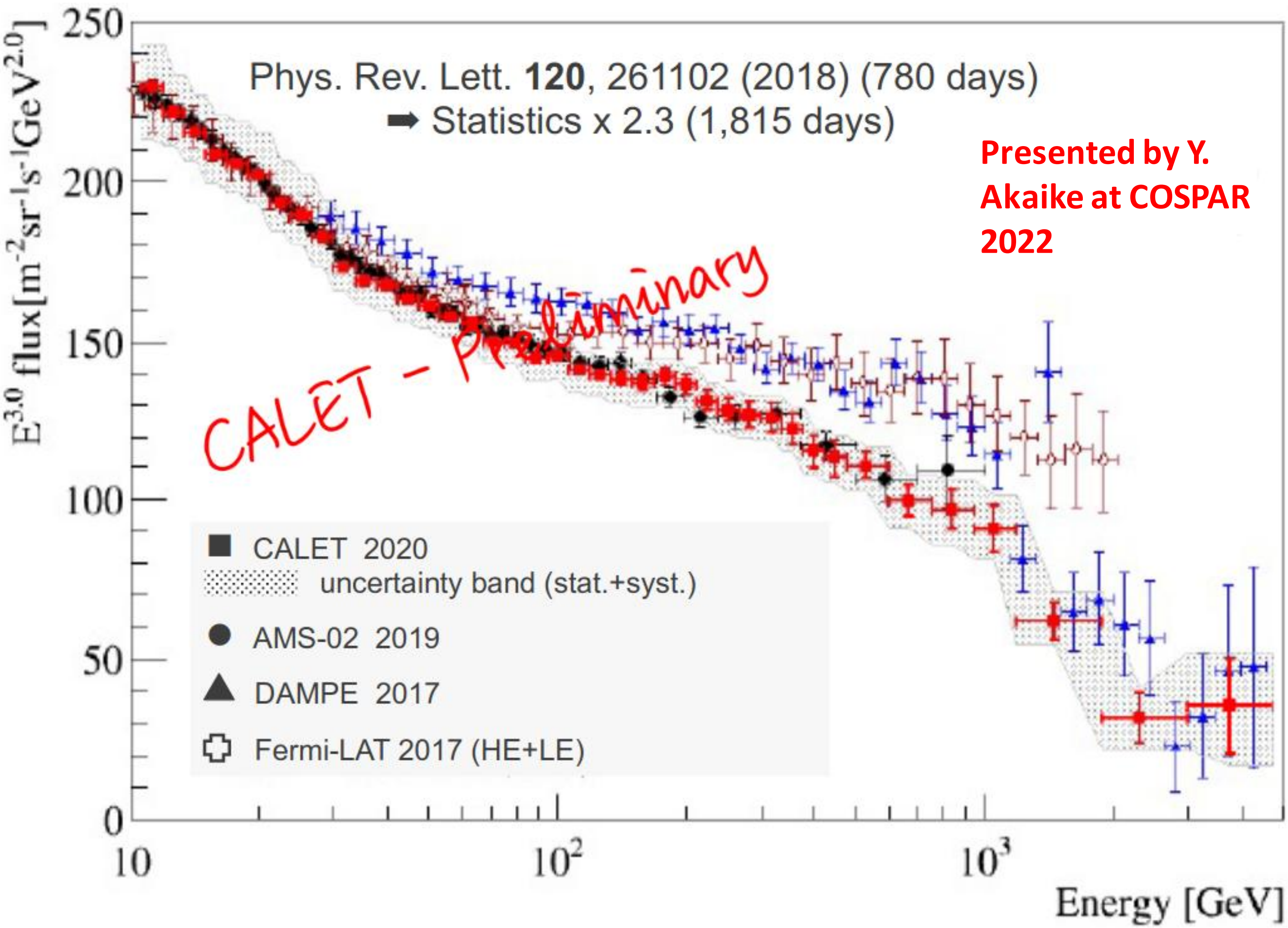

Modeling of contributions from CR electron sources

H. Motz for the CALET Collaboration
ICRC 2021 PoS(ICRC2021)100

Best fit | **95% C.L.**

Vela

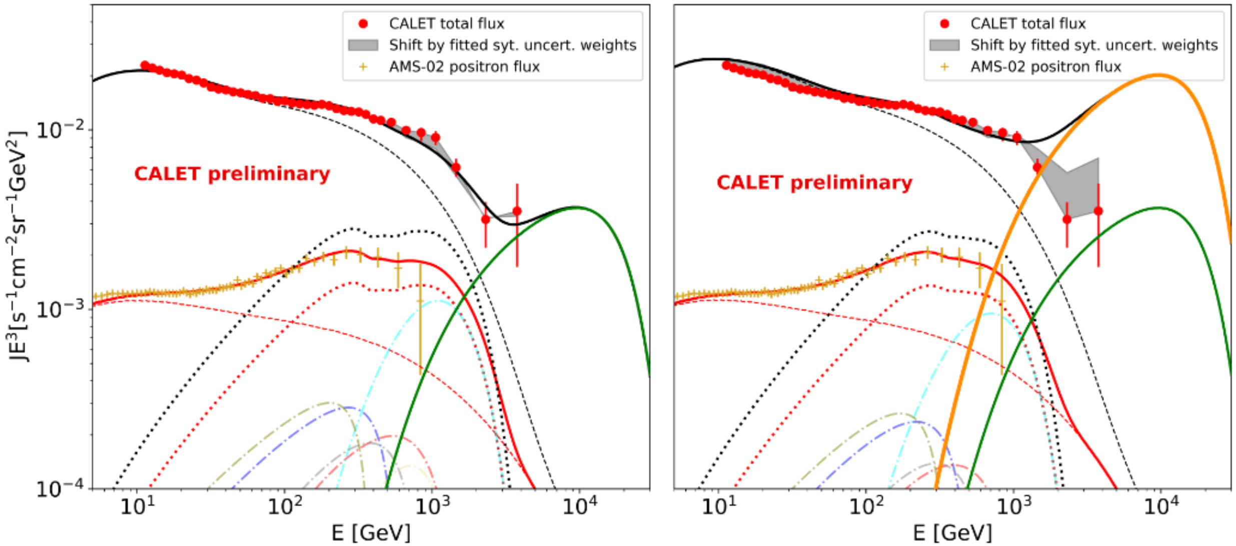

Left: Best Fit (χ^2/ndof = 35.8/76.0)
Right: Limit Fit (χ^2/ndof = 98.5/77.0):
total flux (CALET $\chi^2_{bestfit}$=20.4 , χ^2_{limit}= 84.0)
background from secondaries and distant SNRs
total flux from all pulsars
positron flux (AMS $\chi^2_{bestfit}$=15.5 , χ^2_{limit}=14.5)
background from secondaries
positron flux from all pulsars, individual pulsars:
J0633+1746 [Geminga]
J0659+1414 [Monogem]
J0940-5428
J1003-4747
J1057-5226
electron flux from local SNRs:
Vela-SNR limit fit
Vela-SNR best fit

SNR parameters
Injection spectrum power law index: $\gamma_{i_{SNR}}$ = 2.335
Injection spectrum cutoff energy: $E_{cut_{SNR}}$ = 30 TeV
Cosmic-ray injection timing : delay: 5000 yr duration: 0 yr
Best-fit value for emitted energy: $Q_{0_{SNR}}$ = 2.08 10^{48}erg
95%CL limit on emitted energy: $Q_{0_{SNR}}$ = 11.42 10^{48}erg

Vela + Monogem + Cygnus Loop

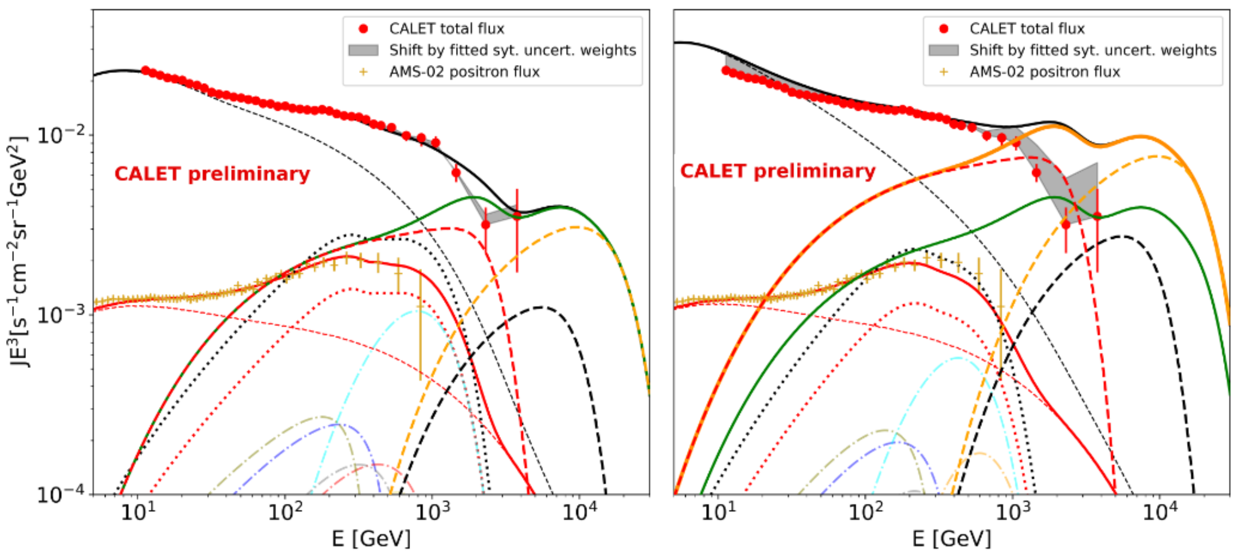

Left: Best Fit (χ^2/ndof = 31.0/76.0)
Right: Limit Fit (χ^2/ndof = 98.5/77.0):
total flux (CALET $\chi^2_{bestfit}$=15.6 , χ^2_{limit}= 80.1)
background from secondaries and distant SNRs
total flux from all pulsars
positron flux (AMS $\chi^2_{bestfit}$=15.4 , χ^2_{limit}=18.4)
background from secondaries
positron flux from all pulsars, individual pulsars:
J0633+1746 [Geminga]
J0835-4510 [Vela]
J0940-5428
J1003-4747
J1057-5226
electron flux from local SNRs:
Combined local SNR limit fit
Combined local SNR best fit
Vela-SNR
CygnusLoop
Monogem-SNR

SNR parameters
Injection spectrum power law index: $\gamma_{i_{SNR}}$ = 2.335
Injection spectrum cutoff energy: $E_{cut_{SNR}}$ = 30 TeV
Cosmic-ray injection timing : delay: 5000 yr duration: 0 yr
Best-fit value for emitted energy: $Q_{0_{SNR}}$ = 1.74 10^{48}erg
95%CL limit on emitted energy: $Q_{0_{SNR}}$ = 4.31 10^{48}erg

CR Electrons summary

- Cosmic-ray electrons are a unique channel for probing acceleration in nearby SNRs and dark matter candidates with decay via leptonic channels
- Current generation instruments are providing precision measurements of the electron spectrum into the TeV energy range
  - Calorimeters such as CALET, DAMPE, and Fermi-LAT provide direct sampling of the EM shower energy to provide accurate energy measurements
  - Magnetic spectrometers (see J. Mitchell's talk earlier today) such as AMS-02 and PAMELA offer charge-sign discrimination as well
- These current measurements are constraining structure in the spectrum, but significant questions remain
  - What systematic effects underlie the discrepancy between the flux normalization between CALET/AMS-02 and DAMPE/Fermi-LAT?
  - Are there contributions at energies above a few TeV from nearby SNRs such as Vela, Monogem, and the Cygnus loop?
  - Is the single-bin excess in the DAMPE measurement at ~1.4 a measurement artifact or a real signal?
  - Will higher-energy measurements reveal CR electron anisotropy?